Supporting Information

Multistimuli-Responsive Dual-State Emissive Imidazo[1,2-α]pyridine as Imaging Probe for Lipid Droplets

Yu Yuan[1,†], Xinran Zhao[1,†], Yueli Zhao[2], Wenjing Zhang[1], Shuai Lu[1,*], Bing Song[2,*], Xinju Zhu[1,*], Xin-Qi Hao[1,*],& Shuang-Quan Zang[1]

[1]*College of Chemistry, Pingyuan Laboratory, Zhengzhou University, No. 100 of Science Road, Henan, Zhengzhou, 450001, P. R. China*

[2]*School of Life Sciences, Zhengzhou University, No. 100 of Science Road, Henan, Zhengzhou, 450001, P. R. China*

Table of Contents

1. Synthesis

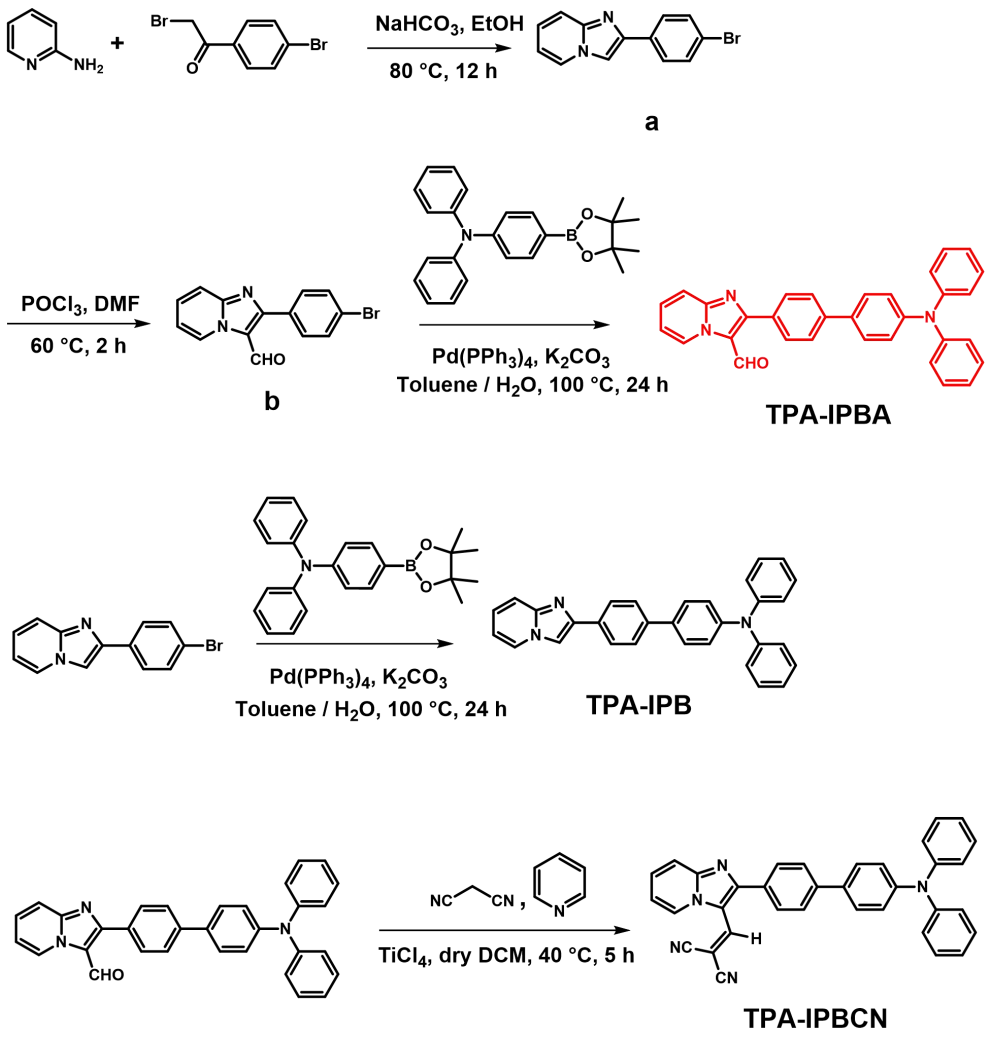

Scheme. S1. The synthetic route for **TPA-IPB**, **TPA-IPBA** and **TPA-IPBCN**.

Synthesis of the intermediate *a*. To a 50 mL round-bottom flask, 2-aminopyridine (51.33 mg, 0.54 mmol), para-α-dibromophenone (100 mg, 0.36 mmol), and sodium bicarbonate (45.37 mg, 0.54 mmol) were added. Subsequently, 1 mL of CH_3CN/H_2O = 9/1 was added. The mixture was refluxed at 80°C for 1 h. After the reaction is complete, pour it into three times water and quench it, the mixture was extracted with ethyl acetate for three times. The collected organic layer was dried over Na_2SO_4, and the solvents were evaporated under vacuum. The residue was purified by column churomatography on silica gel with ether/ethyl acetate (2:1) as eluent to afford a yellow solid (91.96 mg). Yield: 93%. ^{1}H NMR (600 MHz, $CDCl_3$) δ 8.13 (s, 1H), 8.11 (s, 1H), 7.86 (s, 1H), 7.83 (d, J = 8.4 Hz,

2H), 7.63 (d, *J* = 9.1 Hz, 1H), 7.56 (d, *J* = 8.3 Hz, 2H), 7.21 - 7.16 (m, 1H), 6.80 (t, *J* = 6.7 Hz, 1H).

Synthesis of the intermediate *b*. To a 50 mL round-bottom flask intermediate **a** (100 mg, 0.37 mmol) and DMF (1.2 mL) under ice bath conditions were added. Subsequently, drip $POCl_3$ (56.43 mg), after the addition, the reaction was carried out at 60°C for 2 h. After the reaction is complete, add three times the amount of water to quench, stir overnight, DCM (100 mL) was added in the mixture for extraction. The collected organic layer was dried over Na_2SO_4, and the solvents were evaporated under vacuum. The residue was purified by column churomatography on silica gel with ether/ethyl acetate (v/v = 5/1) as the eluent to afford a white solid (113.0 mg). Yield: 98% .^{1}H NMR (600 MHz, $CDCl_3$) δ 10.05 (s, 1H), 9.66 (d, *J* = 6.8 Hz, 1H), 7.81 (d, *J* = 8.9 Hz, 1H), 7.72 (d, *J* = 8.4 Hz, 2H), 7.68 (d, *J* = 8.4 Hz, 2H), 7.64 - 7.57 (m, 1H), 7.15 (t, *J* = 6.9 Hz, 1H).

Synthesis of *TPA-IPB*. To ***a*** 100 mL Schlenk flask, compound a (150 mg, 0.55 mmol), TPA boronic ester (186 mg, 0.55 mmol), $Pd(PPh_3)_4$ (29 mg, 0.028 mmol), and K_2CO_3 (207 mg, 1.65 mmol) were added. Subsequently, toluene/H_2O (20 mL, v/v = 4:1) were added. After refluxed for 24 h under Ar, the reaction mixture was cooled to room temperature and extracted with DCM (30 mL × 3). The combined organic layer was dried over anhydrous Na_2SO_4 and concentrated. The residue was purified by column churomatography on silica gel with ether/ethyl acetate (v/v = 2/1) as the eluent to afford **TPA-IPB** as a yellow solid (154 mg). Yield: 71%. ^{1}H NMR (600 MHz, $CDCl_3$) δ 8.14 (d, *J* = 6.7 Hz, 1H), 8.01 (d, *J* = 8.3 Hz, 2H), 7.90 (s, 1H), 7.66 (t, *J* = 7.8 Hz, 3H), 7.54 (d, *J* = 8.6 Hz, 2H), 7.28 (d, *J* = 8.0 Hz, 4H), 7.20 - 7.17 (m, 1H), 7.15 (dd, *J* = 8.1, 4.2 Hz, 6H), 7.04 (t, *J* = 7.3 Hz, 2H), 6.79 (t, *J* = 6.7 Hz, 1H). ^{13}C NMR (151 MHz, $CDCl_3$) δ 147.70, 147.28, 145.78, 145.62, 140.12, 134.67, 132.29, 129.30, 127.61, 126.87, 126.45, 125.56, 124.64, 124.45, 123.94, 122.96, 117.57, 112.43, 108.11. HRMS (ESI) m/z calcd for [$C31H24N3^+$] 438.1965 ([M+H]$^+$); found 438.1965.

Synthesis of *TPA-IPBCN*. To a 50 mL three-necked round-bottom flask, **TPA-IPBA** (80 mg, 0.17 mmol) and malononitrile (40 mg, 0.52 mmol) in dry DCM (5 mL) at 0°C under Ar. $TiCl_4$ (73 mg, 0.43 mmol) in dry DCM (5 mL) was slowly added, and the mixture was

stirred at 0°C for another 30 min. Pyridine (177 mg, 2.24 mmol) in dry DCM (10 mL) was added dropwise afterwards at 0°C. After that, the solution was allowed to be refluxed for another 3 h. After cooled down to room temperature, the mixture was poured into water (30 mL) and extracted with DCM (30 mL × 3). The combined organic layer was dried over anhydrous Na_2SO_4 and concentrated. The residue was purified by column churomatography on silica gel with ether/ethyl acetate (v/v = 2/1) as the eluent to afford **TPA-IPBCN** as an orange solid (50 mg). Yield: 57%. ^{1}H NMR (600 MHz, $CDCl_3$) δ 8.54 (d, *J* = 6.9 Hz, 1H), 7.95 (s, 1H), 7.87 (d, *J* = 8.9 Hz, 1H), 7.76 (dd, *J* = 20.0, 8.3 Hz, 4H), 7.66 - 7.63 (m, 1H), 7.56 (d, *J* = 8.6 Hz, 2H), 7.32 - 7.27 (m, 5H), 7.17 (t, *J* = 7.6 Hz, 6H), 7.06 (t, *J* = 7.4 Hz, 2H). ^{13}C NMR (151 MHz, $CDCl_3$) δ 157.25, 150.21, 148.03, 147.52, 143.64, 142.73, 133.32, 130.62, 130.17, 129.38, 128.95, 127.85, 127.25, 124.74, 123.52, 123.29, 118.60, 116.98, 115.07 (d, *J* = 4.3 Hz), 113.85. HRMS (ESI) m/z calcd for [C35H24N5$^+$] 514.2026 ([M+H]$^+$), found 514.2021.

2. Structure Characterizations.

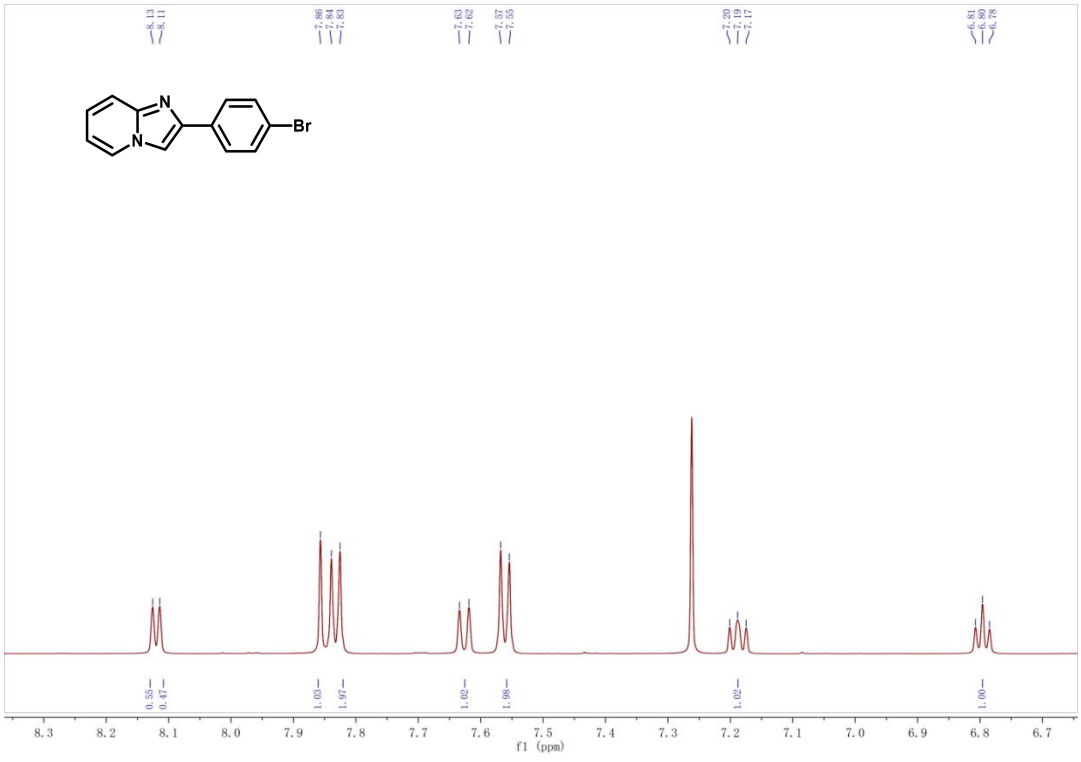

Figure. S1. ^{1}H NMR spectrum (600 MHz) of **a** in $CDCl_3$.

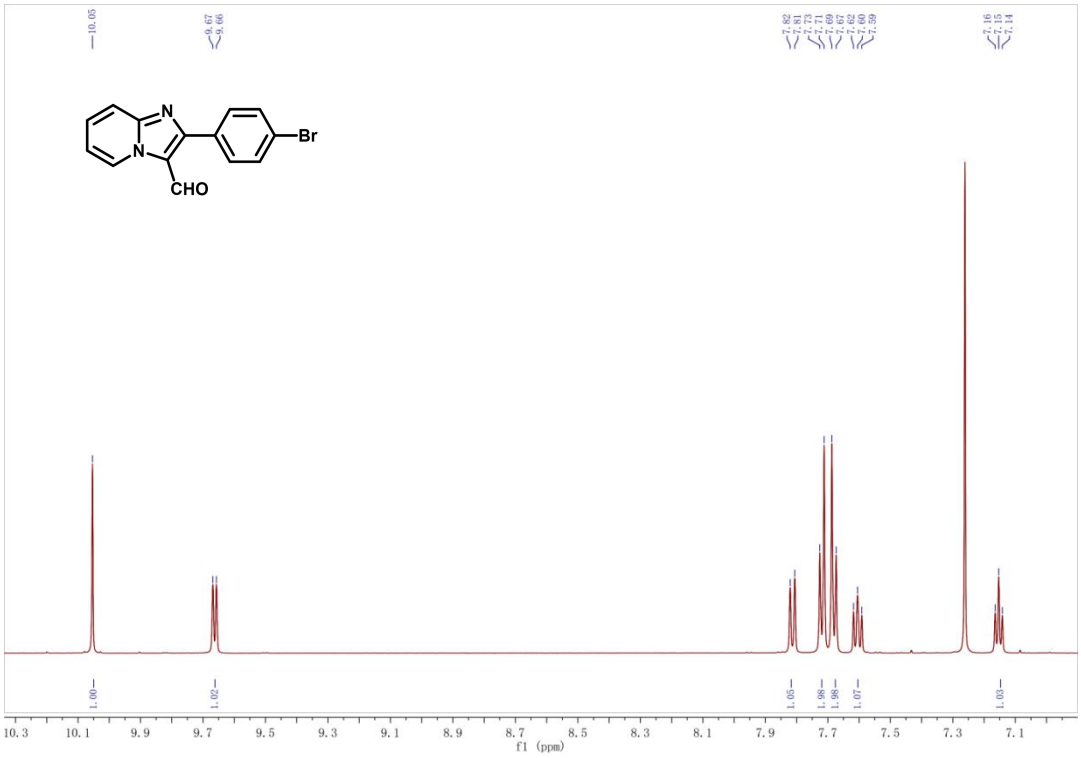

Figure. S2. ^{1}H NMR spectrum (600 MHz) of **b** in $CDCl_3$.

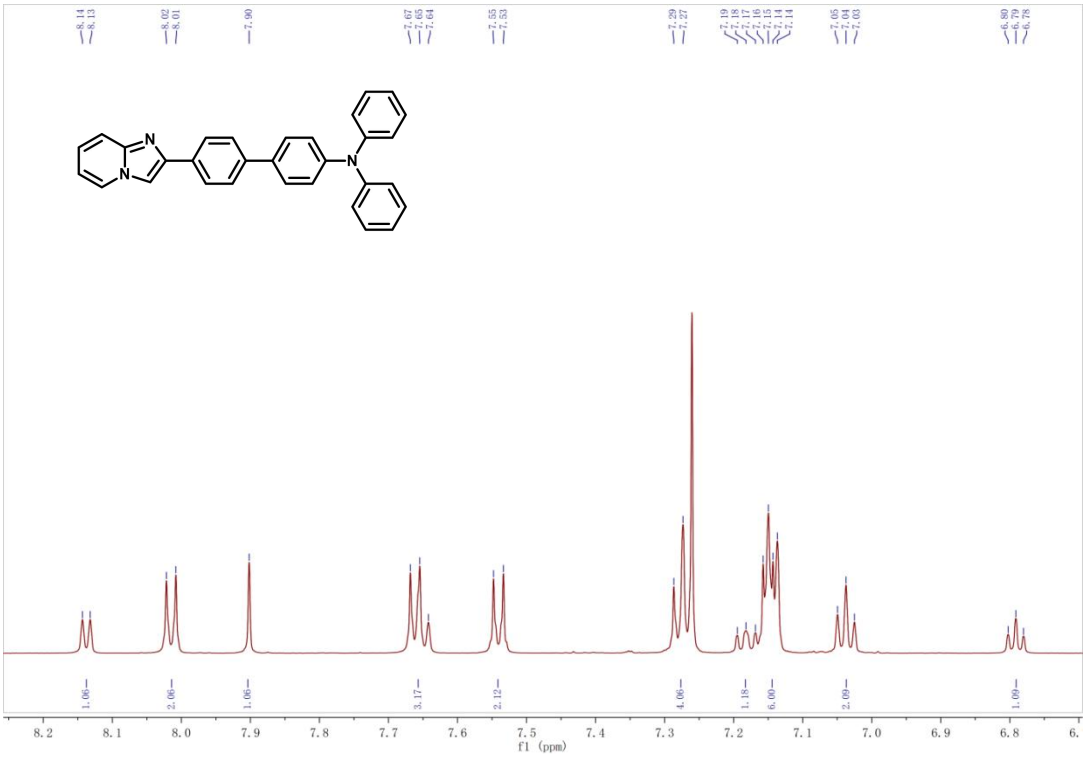

Figure. S3. ^{1}H NMR spectrum (600 MHz) of **TPA-IPB** in $CDCl_3$.

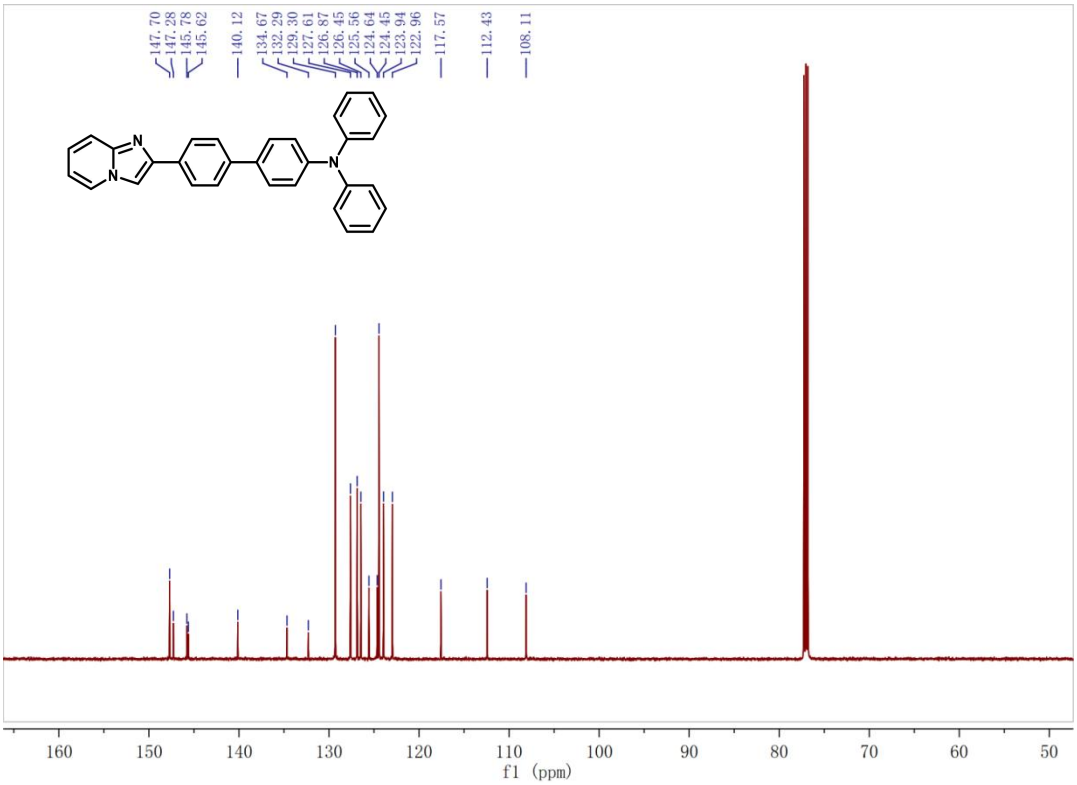

Figure. S4. ^{13}C NMR spectrum (151 MHz) of **TPA-IPB** in $CDCl_3$.

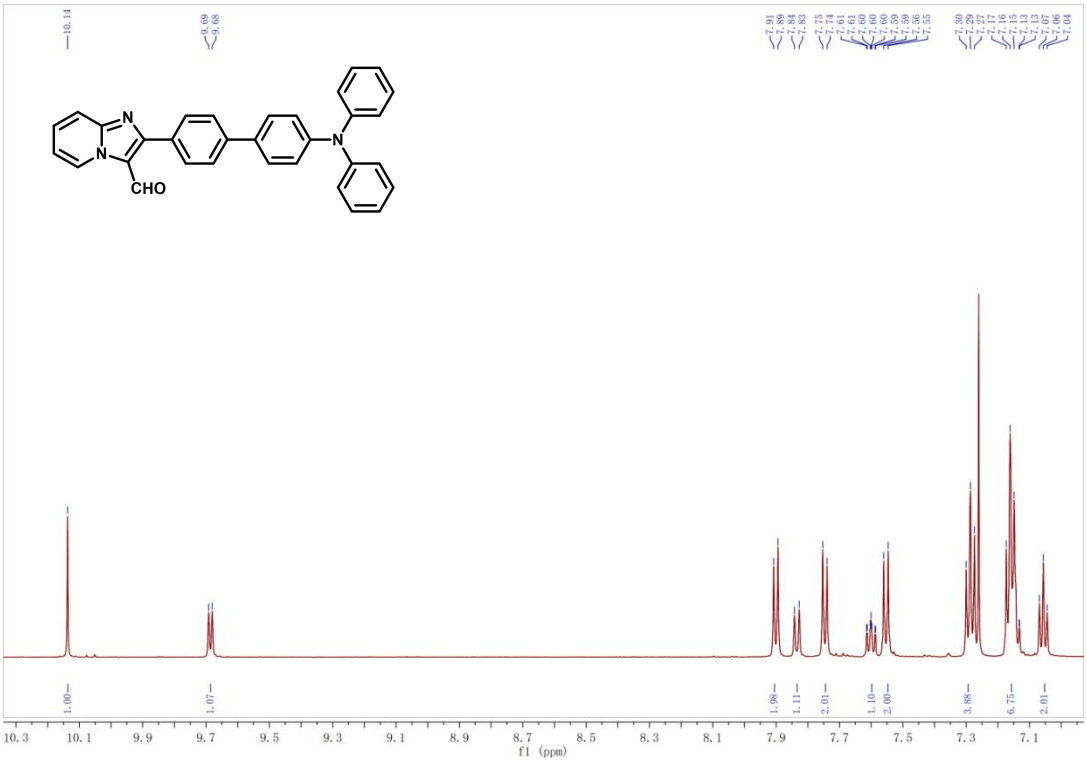

Figure. S5. ^{1}H NMR spectrum (600MHz) of **TPA-IPBA** in $CDCl_3$.

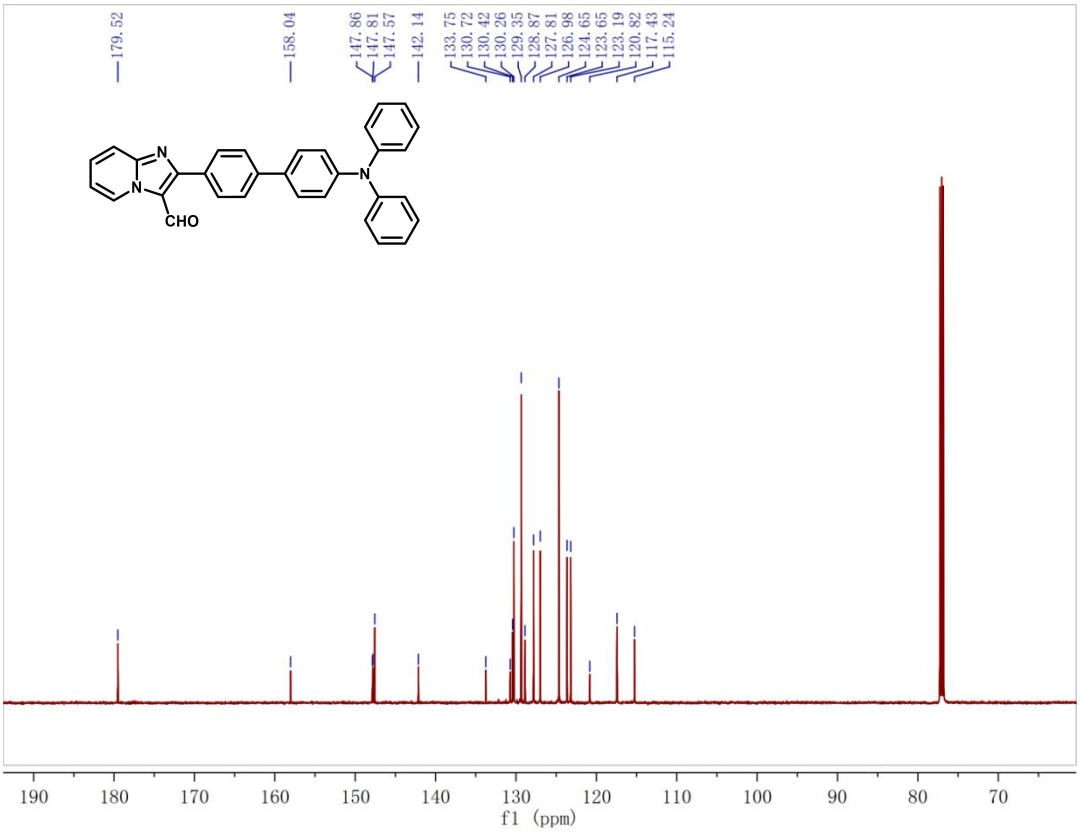

Figure. S6. ^{13}C NMR spectrum (151 MHz) of **TPA-IPBA** in $CDCl_3$.

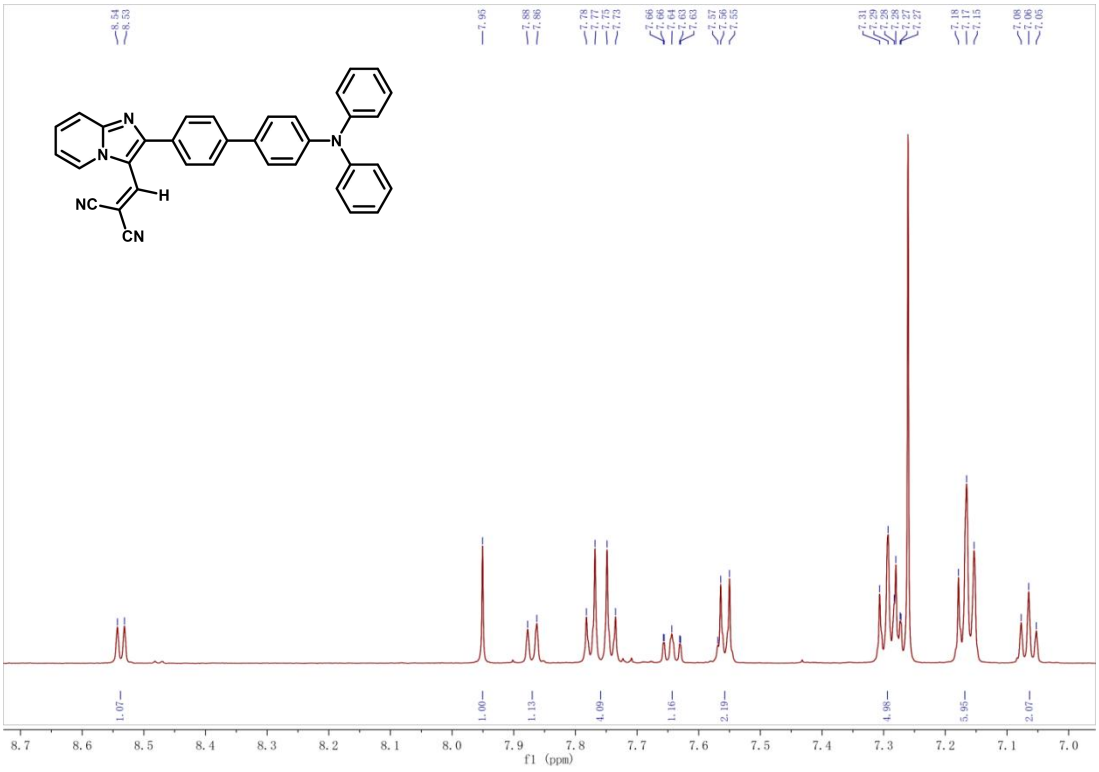

Figure. S7. ^{1}H NMR spectrum (600 MHz) of **TPA-IPBCN** in $CDCl_3$.

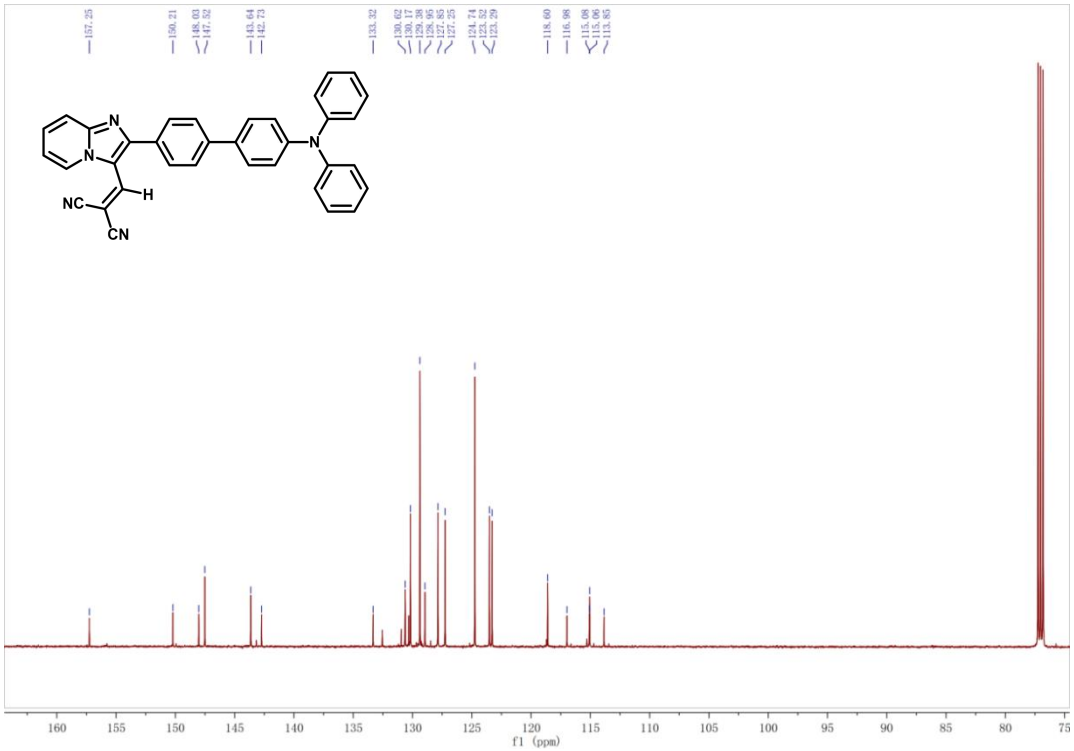

Figure. S8. ^{13}C NMR spectrum (151 MHz) of **TPA-IPBCN** in $CDCl_3$.

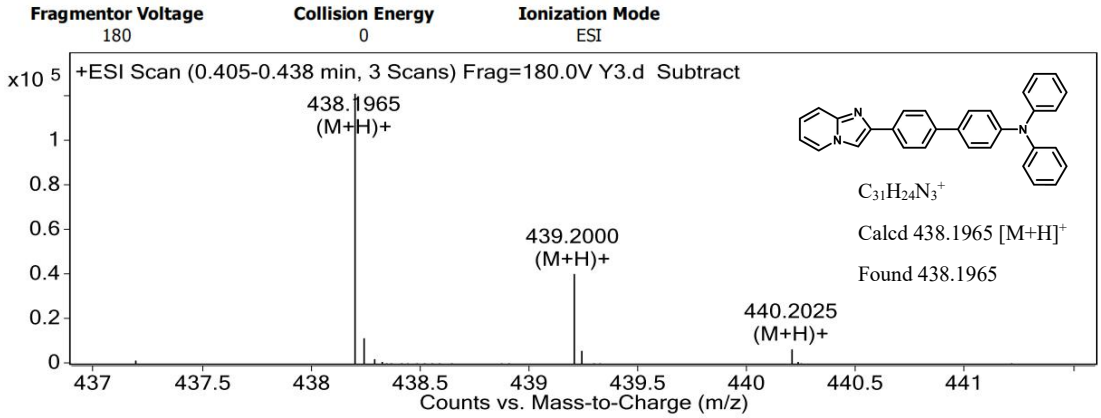

Figure. S9. HRMS spectrum of **TPA-IPB.**

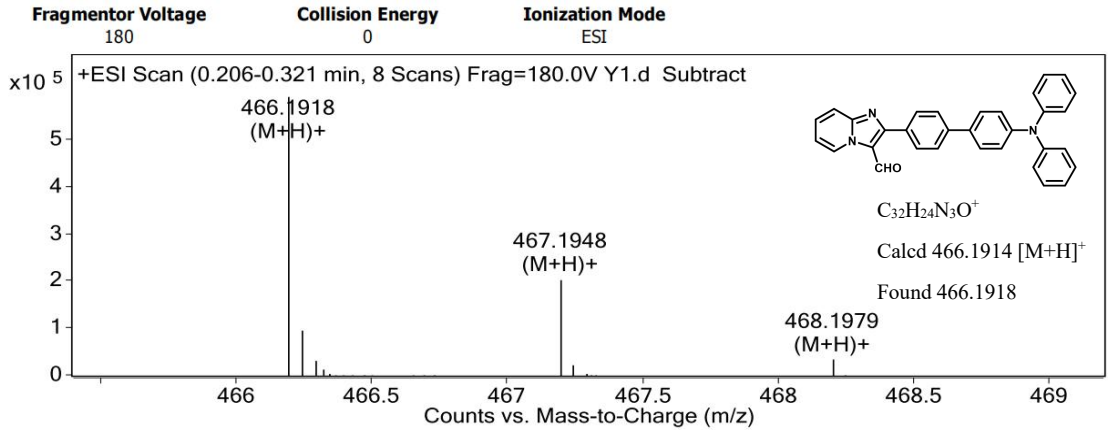

Figure. S10. HRMS spectrum of **TPA-IPBA.**

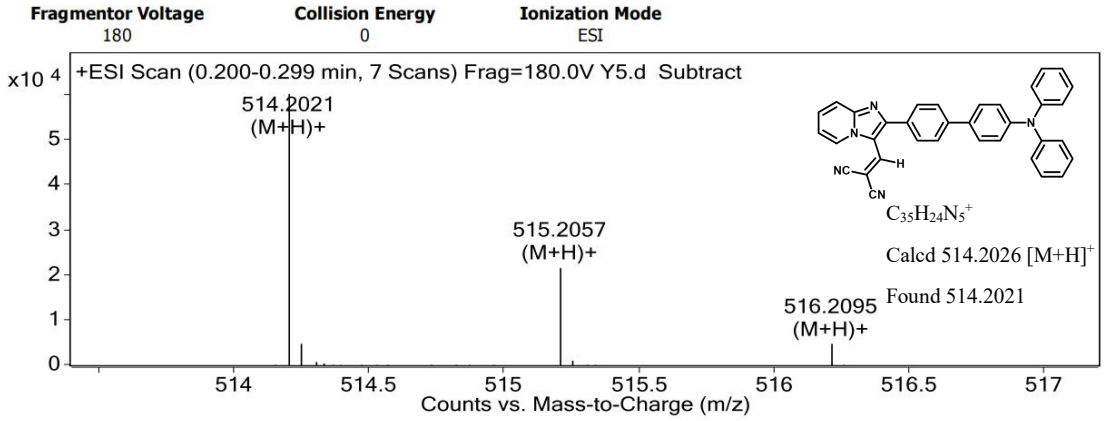

Figure. S11. HRMS spectrum of **TPA-IPBCN.**

3. Photophysical Date

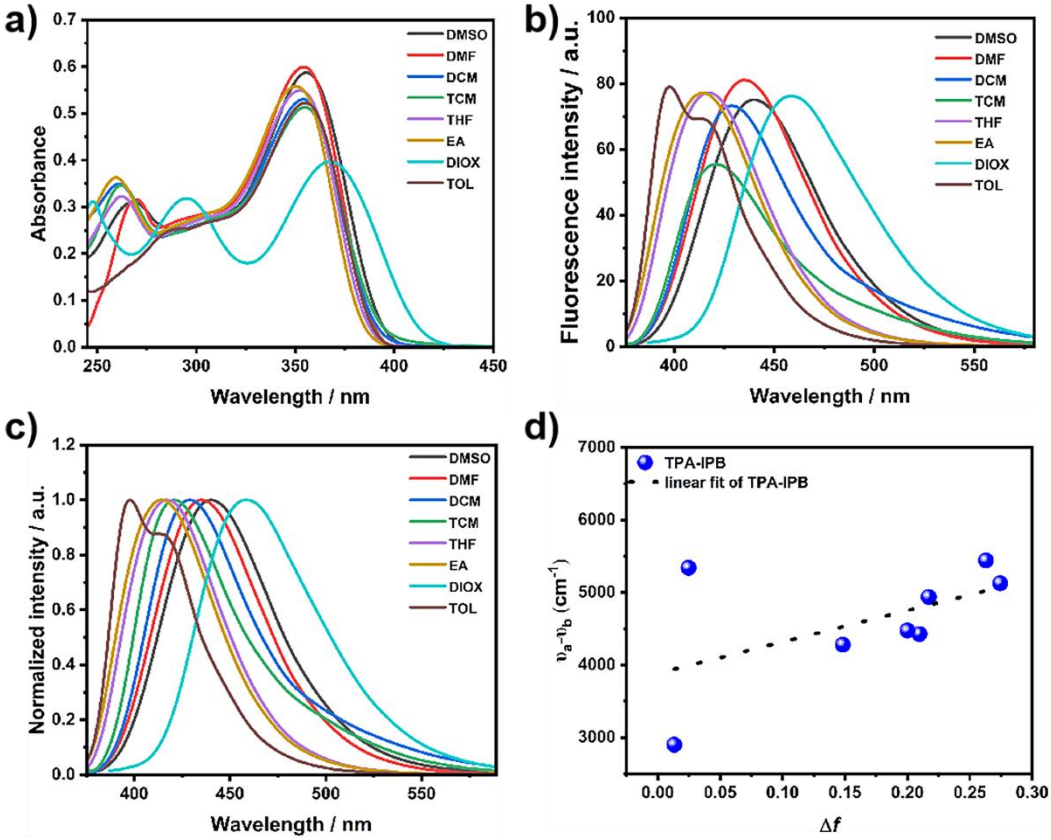

Figure. S12. (a) UV-Vis absorption spectra and (b) emission spectra (c) normalized emission spectra of **TPA-IPB** in different solutions. (d) Linear fitting based on the Lippert-Mataga model in different solvents. The concentration was 10 μM.

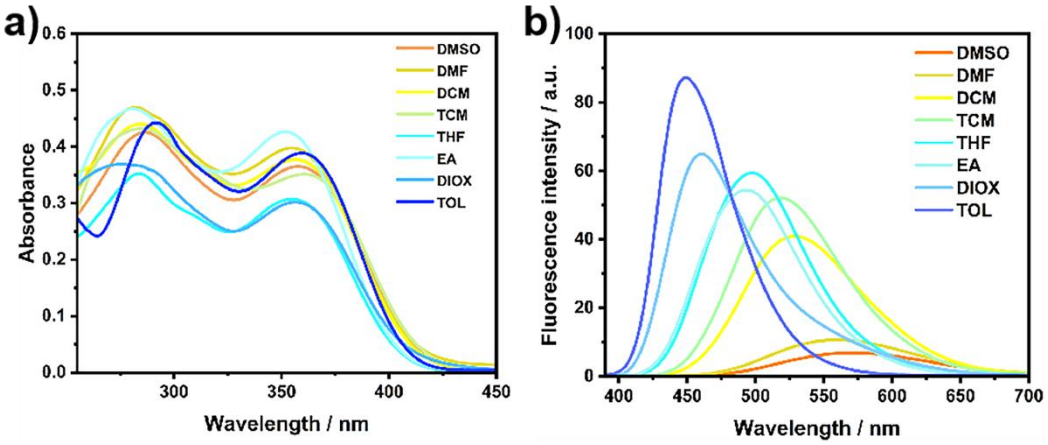

Figure. S13. (a) UV-Vis absorption spectra and (b) emission spectra of **TPA-IPBA** in different solvents. The concentration was 10 μM.

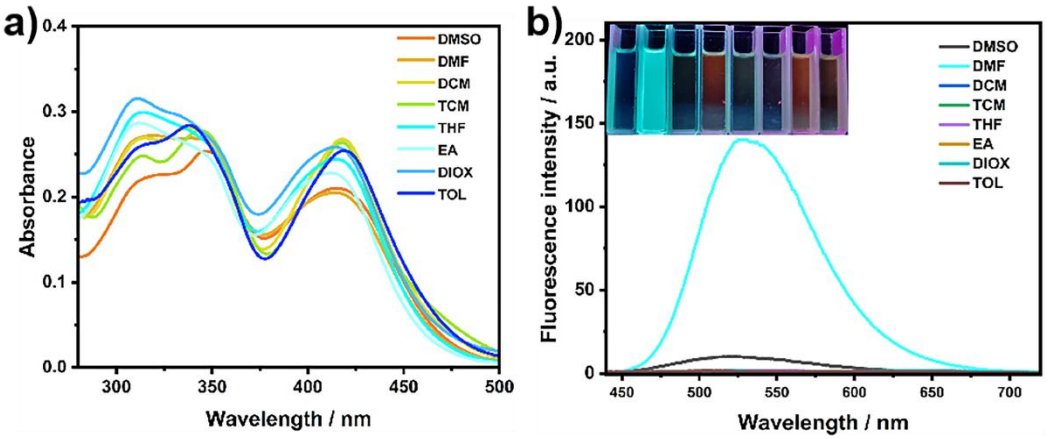

Figure. S14. (a) UV-Vis absorption spectra and (b) emission spectra of **TPA-IPBCN** in different solutions.The illustration is emission color in different solutions excited at 365 nm. The concentration was 10 μM.

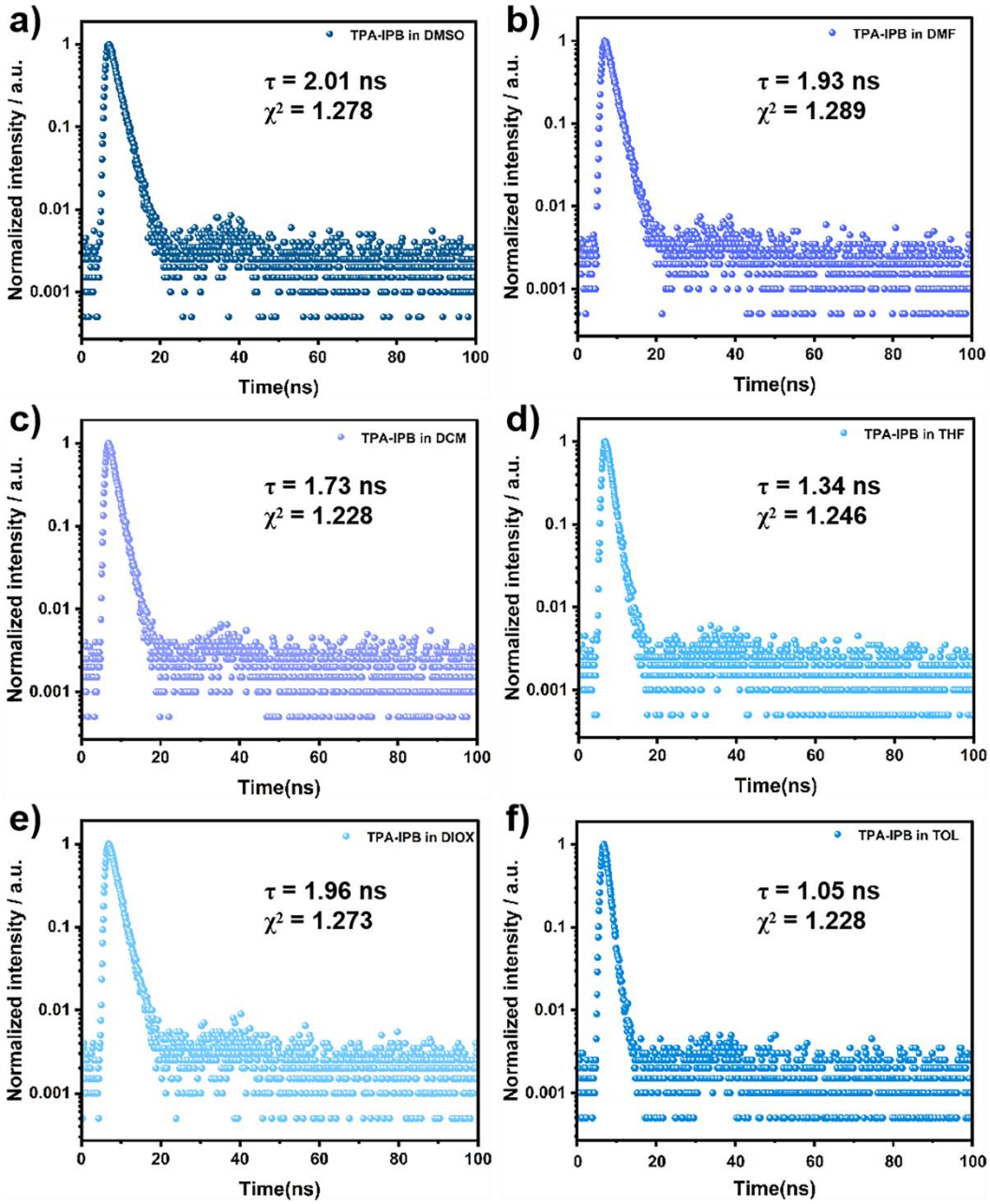

Figure. S15. Fluorescence decay curves of **TPA-IPB** in (a) methyl sulfoxide, (b) N,N-Dimethylformamide, (c) dichloromethane, (d) tetrahydrofuran, (e) 1,4-dioxane, (f) toluene solvents.

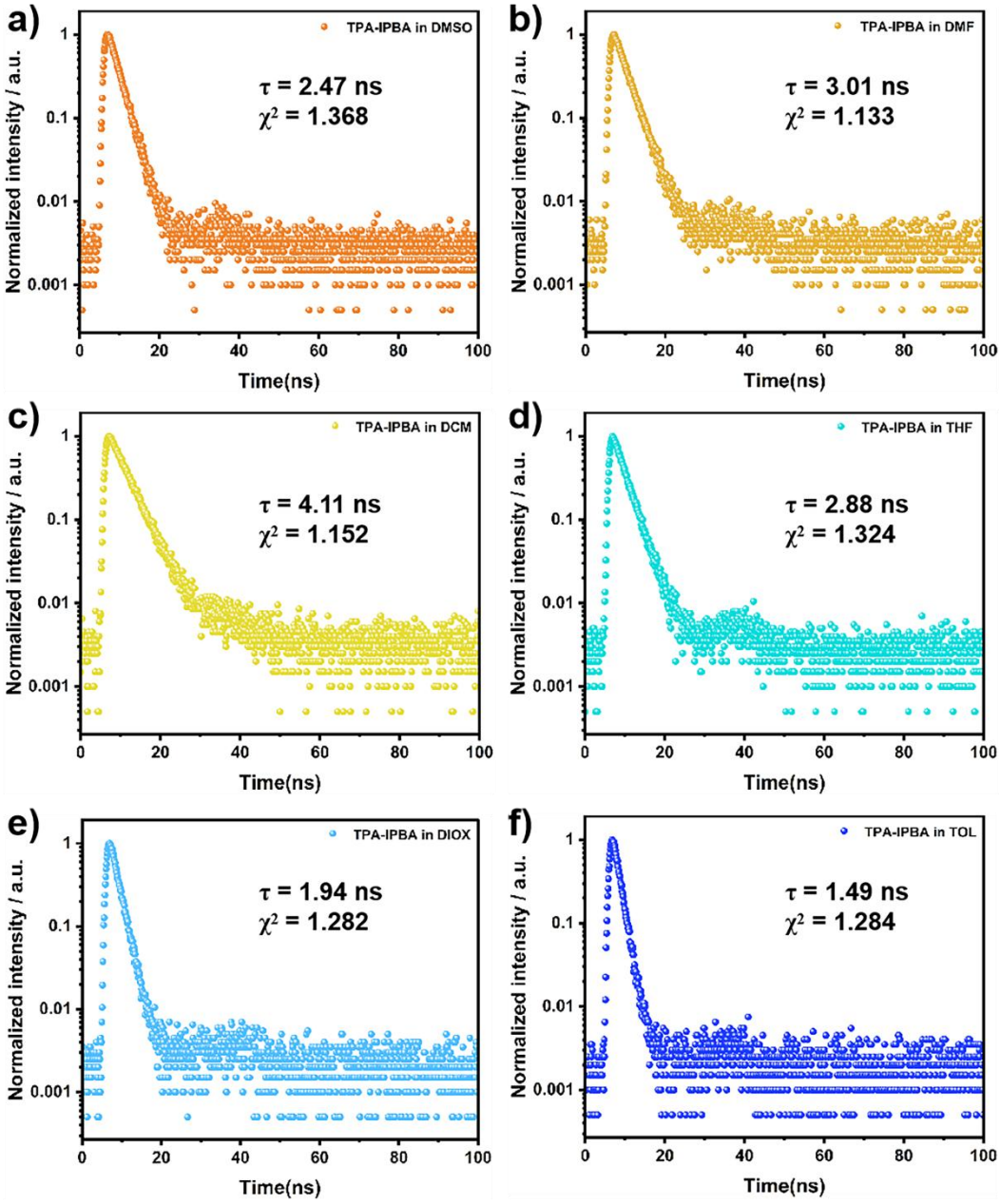

Figure. S16. Fluorescence decay curves of **TPA-IPBA** in (a) methyl sulfoxide, (b) N,N-Dimethylformamide, (c) dichloromethane, (d) tetrahydrofuran, (e) 1,4-dioxane, (f) toluene solvents.

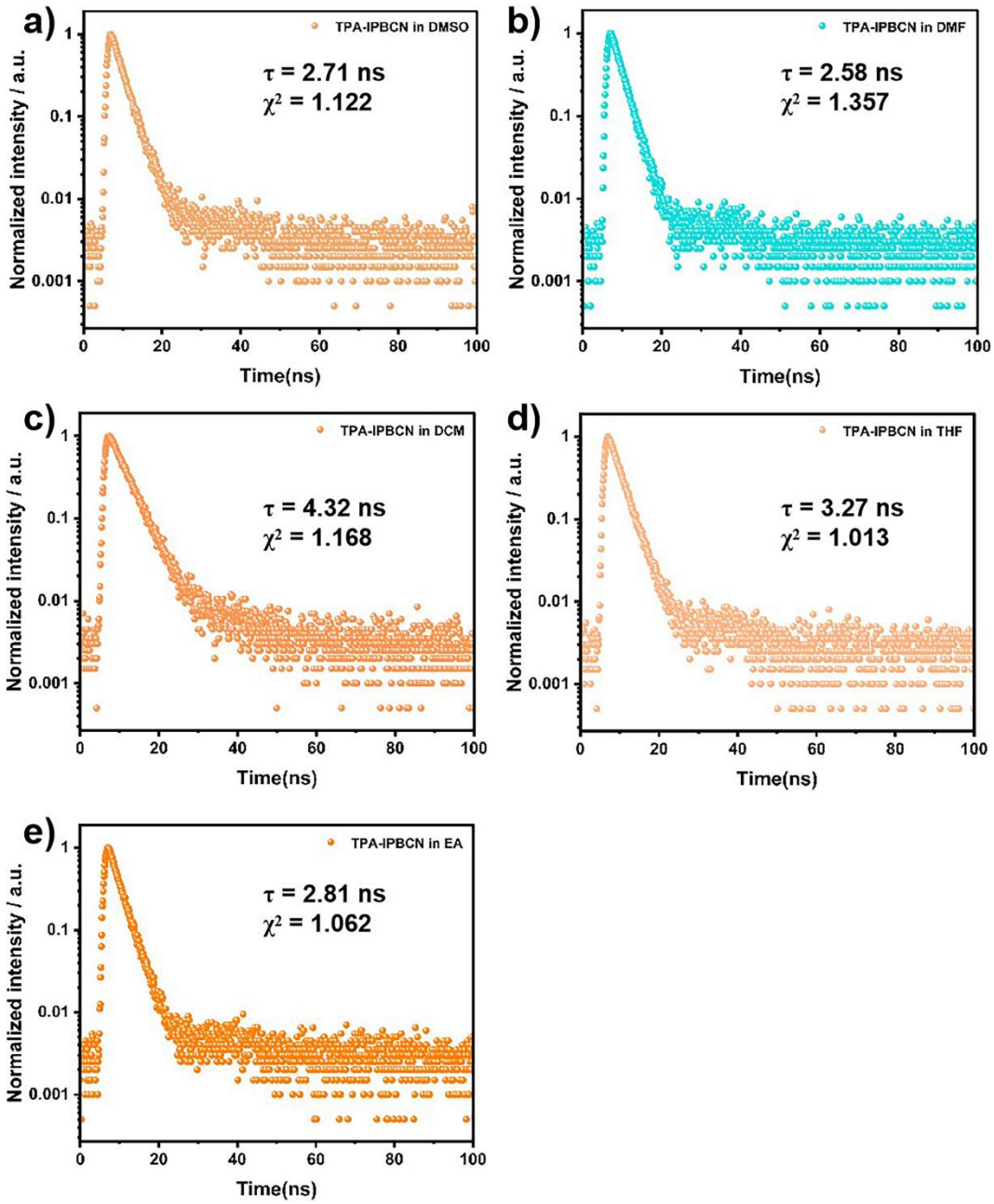

Figure. S17. Fluorescence decay curves of **TPA-IPBCN** in (a) methyl sulfoxide, (b) N,N-Dimethylformamide, (c) dichloromethane, (d) tetrahydrofuran, (e) ethyl acetate solvents.

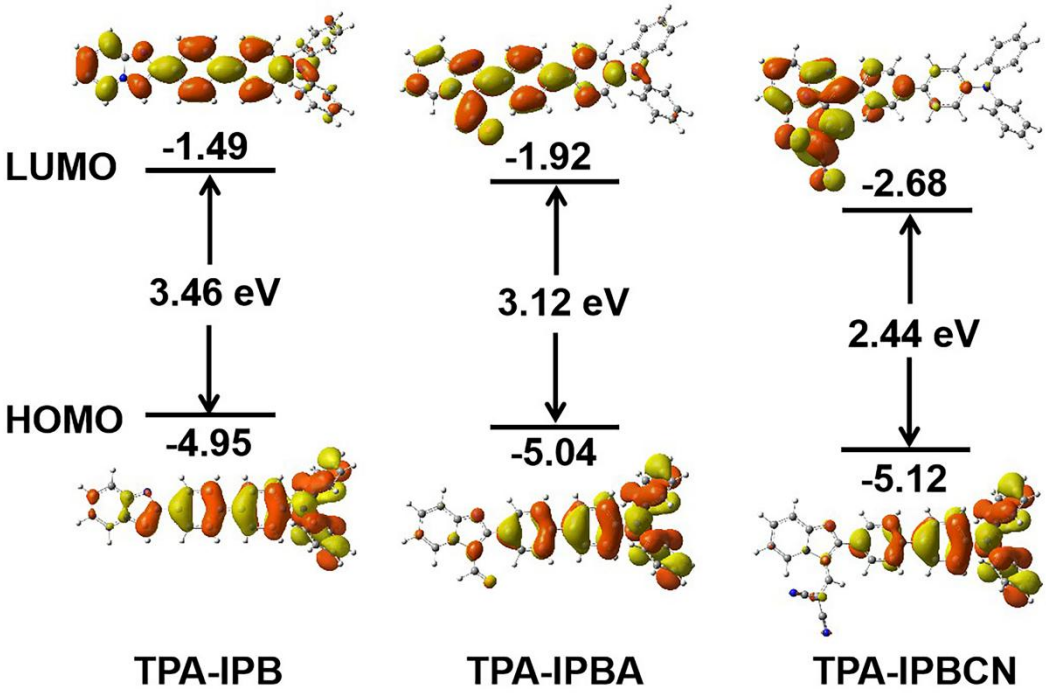

Figure. S18. Frontier molecular orbital energy diagrams corresponding to the dominant transition configuration for the fluorescence emission of **TPA-IPB**, **TPA-IPBA**, and **TPA-IPBCN** in THF solution, respectively. The structures were optimized at the PBE0/6-31G(d, p)/SMD_{THF} level of theory by using the TD-DFT method.

Table S1. Calculated results for vertical excitation, including excitation wavelength (λ_{ex}), oscillator strength (f_{osc}), and transition configurations.

Structures	λ_{ex}/(nm)	f_{osc}	Transition Configurations
TPA-IPB	373.6	1.411	H→L (90.7%) H→L+1 (5.1%)
TPA-IPBA	415.6	0.879	H→L (93.2%) H→L+1 (2.4%) H→L+2 (2.1%)
TPA-IPBCN	514.7	0.314	H→L (97.5%)
TPA-IPBAH$^+$	507.5	0.625	H→L (97.3%)

Table S2. Calculated results for fluorescence emission, including emission wavelength (λ_{em}), oscillator strength (f_{osc}), and transition configurations.

Structures	λ_{em}/(nm)	f_{osc}	Transition Configurations
TPA-IPB	445.6	1.780	H→L (97.0%)
TPA-IPBA	485.8	1.320	H→L (96.1%)
TPA-IPBCN	616.2	0.514	H→L (97.6%)
TPA-IPBAH$^+$	612.7	0.708	H→L (98.4%)

Table S3. Detailed data of **TPA-IPs** for fitting photophysical results in different solvents based on Lippert-Mataga equation.

Sample	Solvent	Δf	λ_{abs}/(nm)	λ_{em}/(nm)	Stokes shift[a](cm^{-1})	Φ_f[b] [%]
TPA-IPB	DMSO	0.26300	268,356	440	5363	89.61
	DMF	0.27438	270,354	436	5313	72.08
	DCM	0.21717	261,354	429	4939	79.71
	THF	0.20964	262,353	417	4348	74.16
	DIOX	0.02465	295,367	459	5461	65.50
	TOL	0.01321	289,355	397	2980	58.31
TPA-IPBA	DMSO	0.26300	287,358	572	10450	30.84
	DMF	0.27438	282,355	559	10280	42.16
	DCM	0.21717	285,357	529	9108	76.68
	THF	0.20964	284,355	497	8048	75.91
	DIOX	0.02465	281,357	460	6272	79.08
	TOL	0.01321	292,360	448	5506	61.48
TPA-IPBCN	DMSO	0.26300	346, 415	521	4903	-
	DMF	0.27438	343, 414	529	5251	1.79
	DCM	0.21717	338, 418	569	6349	-
	TCM	0.14829	344, 418	-	-	-
	THF	0.20964	312, 415	532	5299	0.15
	EA	0.20010	312, 412	540	5753	0.01

[a]Calculated via υ_{abs}-υ_{em}.; [b] Measured in solution state;

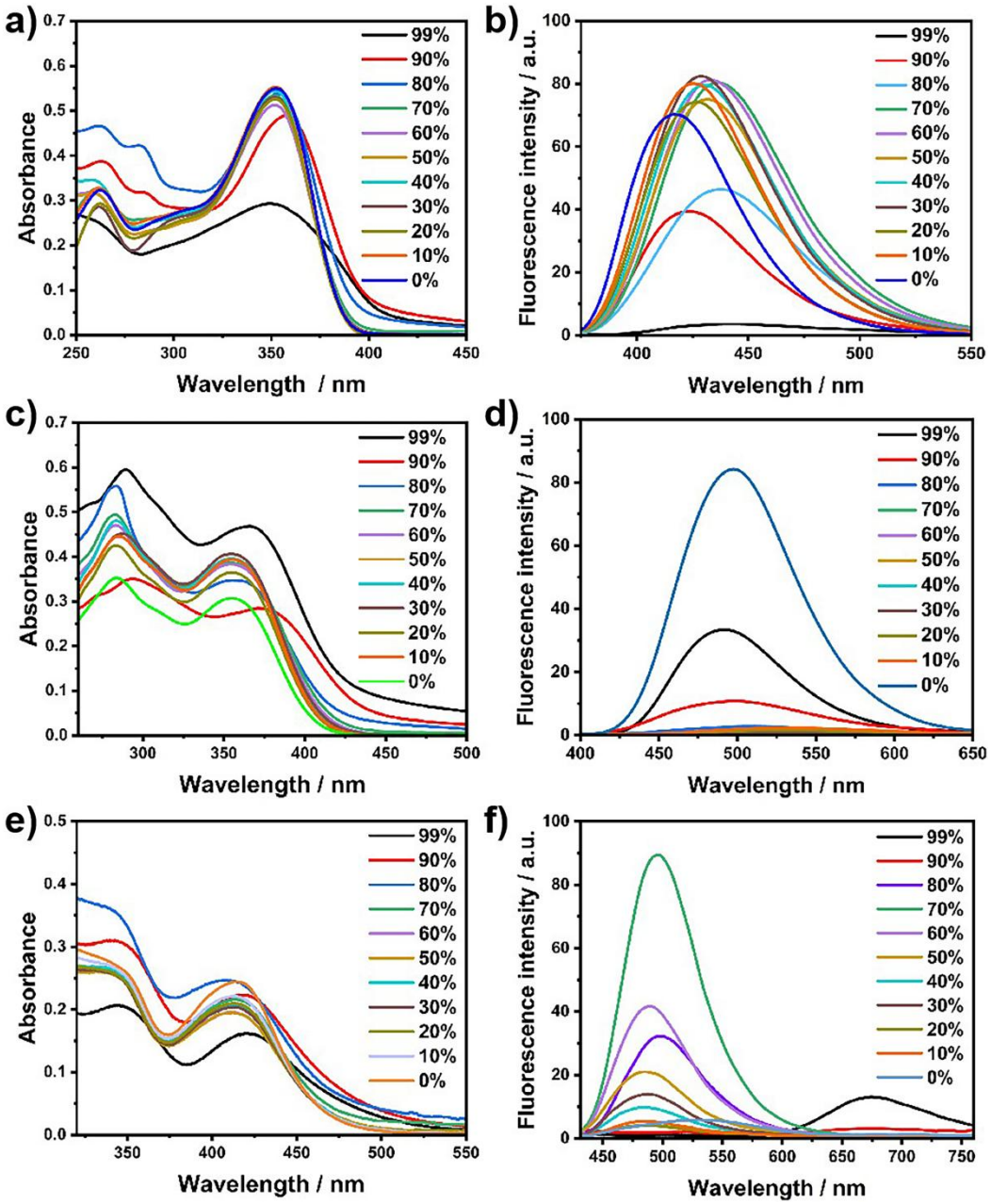

Figure. S19. UV-Vis absorption spectra and emissio spectra of (a, b) **TPA-IPB**, (c, d) **TPA-IPBA**, (e, f) **TPA-IPBCN** in THF/H_2O with different water fractions. The concentration was 10 μM.

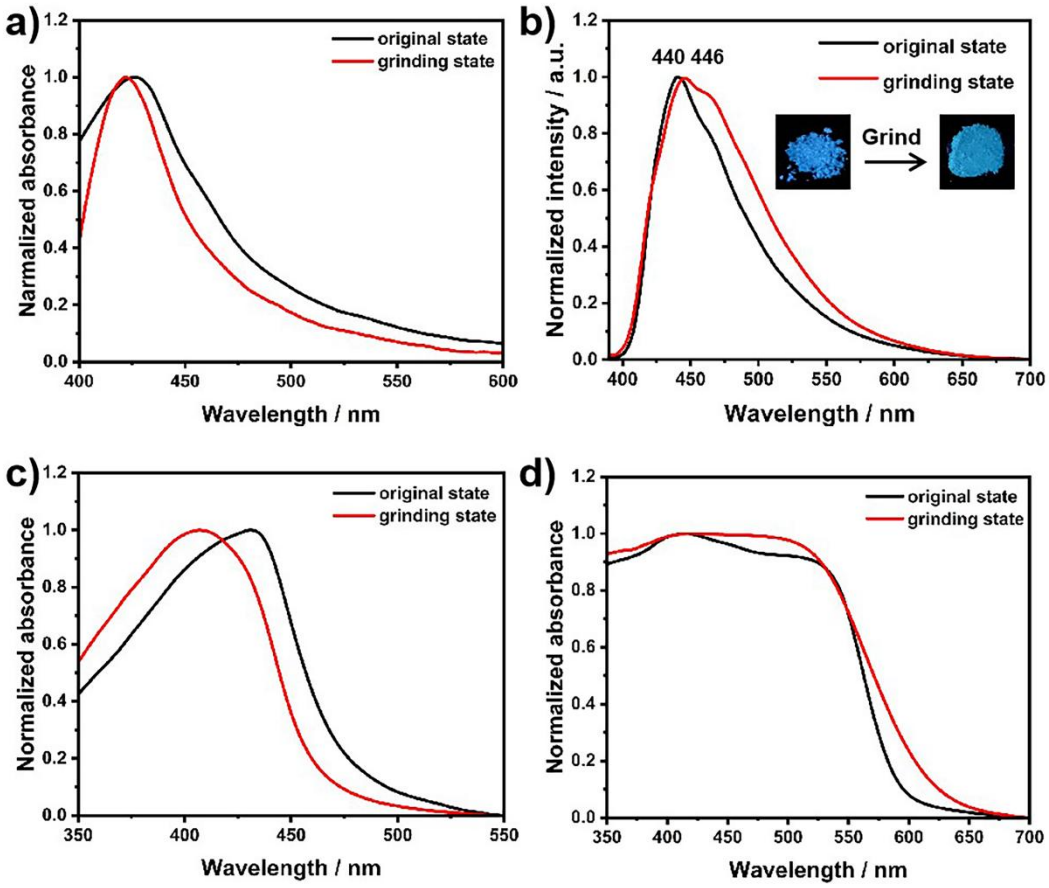

Figure. S20. Noemalized emission spectra of (a) **TPA-IPB**, (b) **TPA-IPBA**, (c) **TPA-IPBCN** and (d) normalized UV-Vis absorption spectra of **TPA-IPB** in different solid states. The illustration is emission color in different solid states excited at 365 nm.

Table S4. Detailed data of **TPA-IPs** in different solid states.

Sample	State	λ_{abs}/(nm)	λ_{em}/(nm)	Φ_f[a] [%]	τ[b](ns)	K_r[c](ns^{-1})	K_{nr}[d](ns^{-1})
TPA-IPB	**Original**	427	440	15.39	2.77	0.056	0.305
	Grinding	420	446	17.31	3.14	0.055	0.263
TPA-IPBA	**Original**	433	462	38.56	3.29	0.117	0.187
	Grinding	408	468	55.42	2.28	0.243	0.196
	DCM	-	494	49.66	3.41	0.146	0.148
	ACN	-	442	33.89	2.22	0.153	0.298
TPA-IPBCN	**Original**	413	608	30.16	18.35	0.016	0.038
	Grinding	422	641	13.73	21.31	0.006	0.040
	Fuming	-	616	5.45	15.63	0.003	0.060

[a]Quantum yield; [b] Fluorescence lifetime; [c] Radiative transition rate constant; [d] Non-radiative transition rate constant.

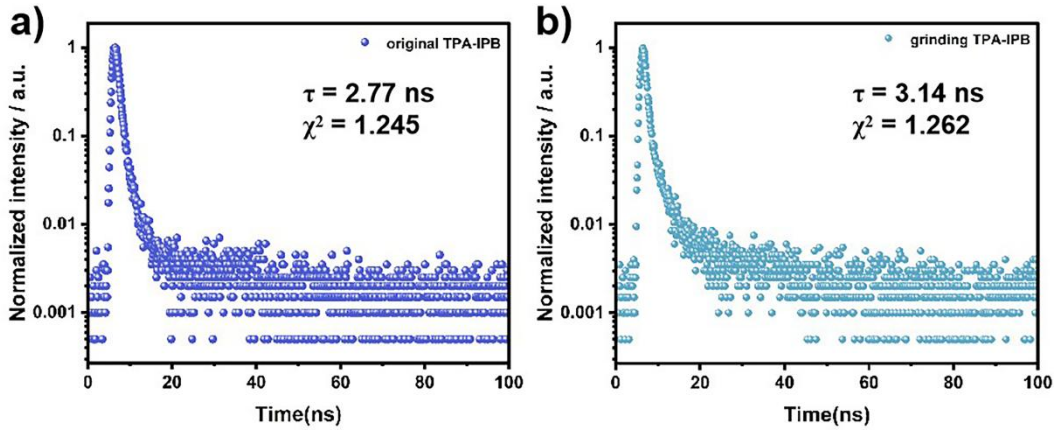

Figure. S21. Fluorescence decay curves of **TPA-IPB** in (a) original solid state, (b) grinding solid state.

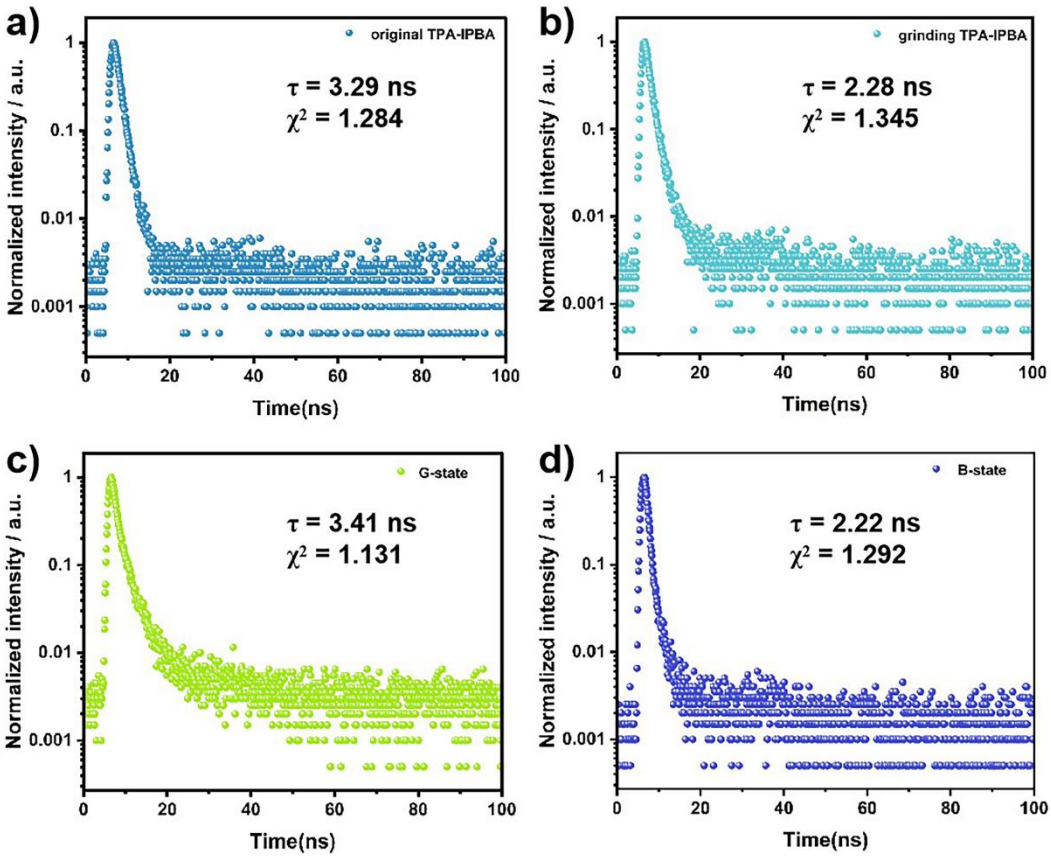

Figure. S22. Fluorescence decay curves of **TPA-IPBA** in (a) original solid state, (b) grinding solid state, (c) G-state, (d) B-state.

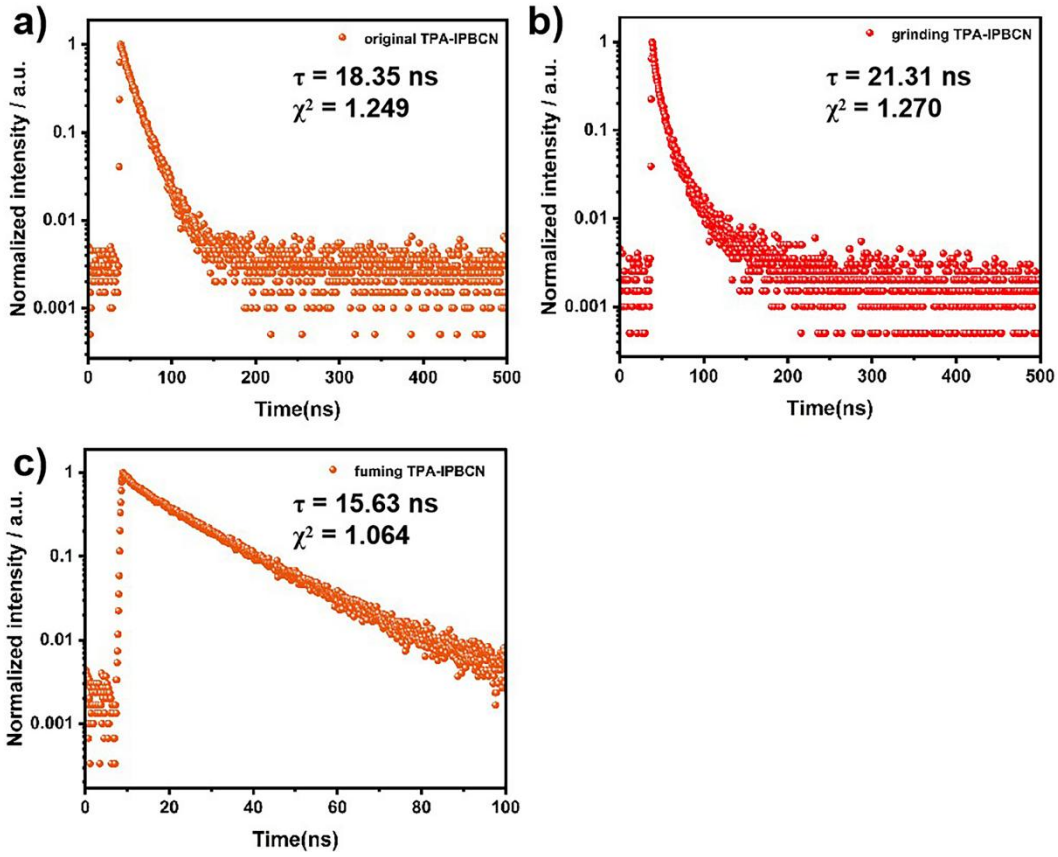

Figure. S23. Fluorescence decay curves of **TPA-IPBCN** in (a) original solid state, (b) grinding solid state, (c) fuming solid state.

4. Crystal data.

Table S5. The crystal data.

Identification code(CCDC)	**TPA-IPB** (2408716)	**B-Type** (2408717)	**G-Type** (2408718)	**O-Type** (2408719)	**R-Type** (2408720)
Empirical formula	$C_{31}H_{23}N_3$	$C_{32}H_{23}N_3O$	$C_{32}H_{23}N_3O$	$C_{35}H_{23}N_5$	$C_{35}H_{23}N_5$
Formula weight	437.55	465.56	465.56	513.60	513.60
Temperature/K	293	293	293	293	293
Crystal system	triclinic	triclinic	monoclinic	monoclinic	monoclinic
Space group	P-1	P-1	C2/c	Cc	Cc
a/Å	10.2097(3)	10.4123(3)	33.0334(4)	24.1308(11)	22.1392(9)
b/Å	16.1966(5)	15.1410(5)	10.24713(14)	19.7012(7)	19.0121(5)
c/Å	16.6730(3)	16.7647(6)	28.4877(3)	7.5359(3)	7.57315(18)
α/°	90.536(2)	82.180(3)	90	90	90
β/°	102.062(2)	88.320(3)	95.6596(12)	113.134(5)	103.137(3)
γ/°	101.221(2)	76.848(3)	90	90	90
Volume/Å3	2641.08(12)	2549.73(15)	9596.0(2)	3294.5(3)	3104.21(18)
Z	4	2	16	4	4
ρcalc/g/cm^3	1.216	1.266	1.289	1.035	1.099
μ/mm^{-1}	0.577	0.611	0.619	0.489	0.519
F(0 0 0)	1024	1020	3904	1072	1072
Crystal size/mm^3	0.18×0.1×0.06	0.15×0.11×0.33	0.15×0.1×0.06	0.16×0.11×0.06	0.19×0.07×0.05
2θ range for data collection/°	3.787 to 67.080	3.754 to 67.075	3.912 to 67.079	3.984 to 67.080	4.101 to 70.320
Reflections collected	20045	34619	17471	13163	11108
Goodness-of-fit on F^2	1.016	1.020	1.024	1.017	1.032
Final R indexes	R_1 = 0.0865, wR_2 = 0.2907	R_1 = 0.0503, wR_2 = 0.1462	R_1 = 0.0505, wR_2 = 0.1450	R_1 = 0.0397, wR_2 = 0.1060	R_1 = 0.0442 wR_2 = 0.1119

Table S6. Dihedral angles in different crystals.

Single crystal/Dihedral angle	θ_1; θ_1'	θ_2; θ_2'	θ_3; θ_3'	θ_4; θ_4'
TPA-IPB	8.722; 8.569	23.043; 5.751	32.220; 45.510	-
B-type	37.098; 46.585	35.304; 22.245	36.734; 47.070	6.724; 6.981
G-type	35.757; 34.716	22.374; 26.784	29.810; 54.456	6.354; 9.897
O-type	29.541	28.204	35.830	42.383
R-type	24.883	31.167	29.125	32.682

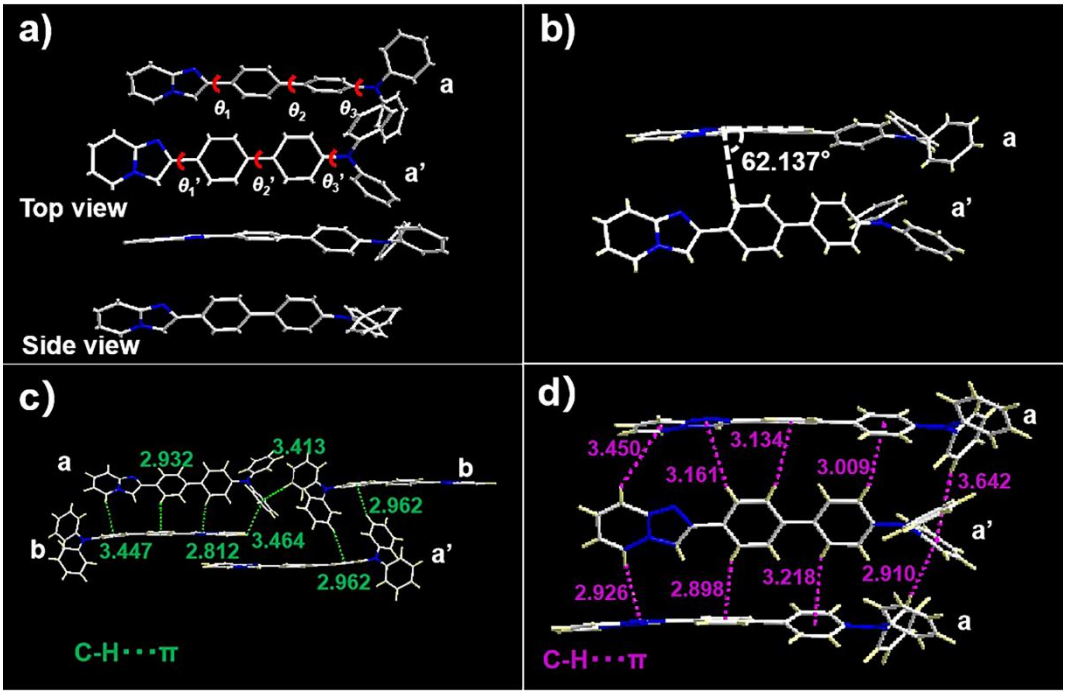

Figure. S24. (a) Single crystal packing patterns of **TPA-IPB**. (b) Packing patterns between the upper and lower layers. (c) Packing patterns and intermolecular forces of paired and adjacent molecules and (d) individual three-layer molecules. Unit: Å.

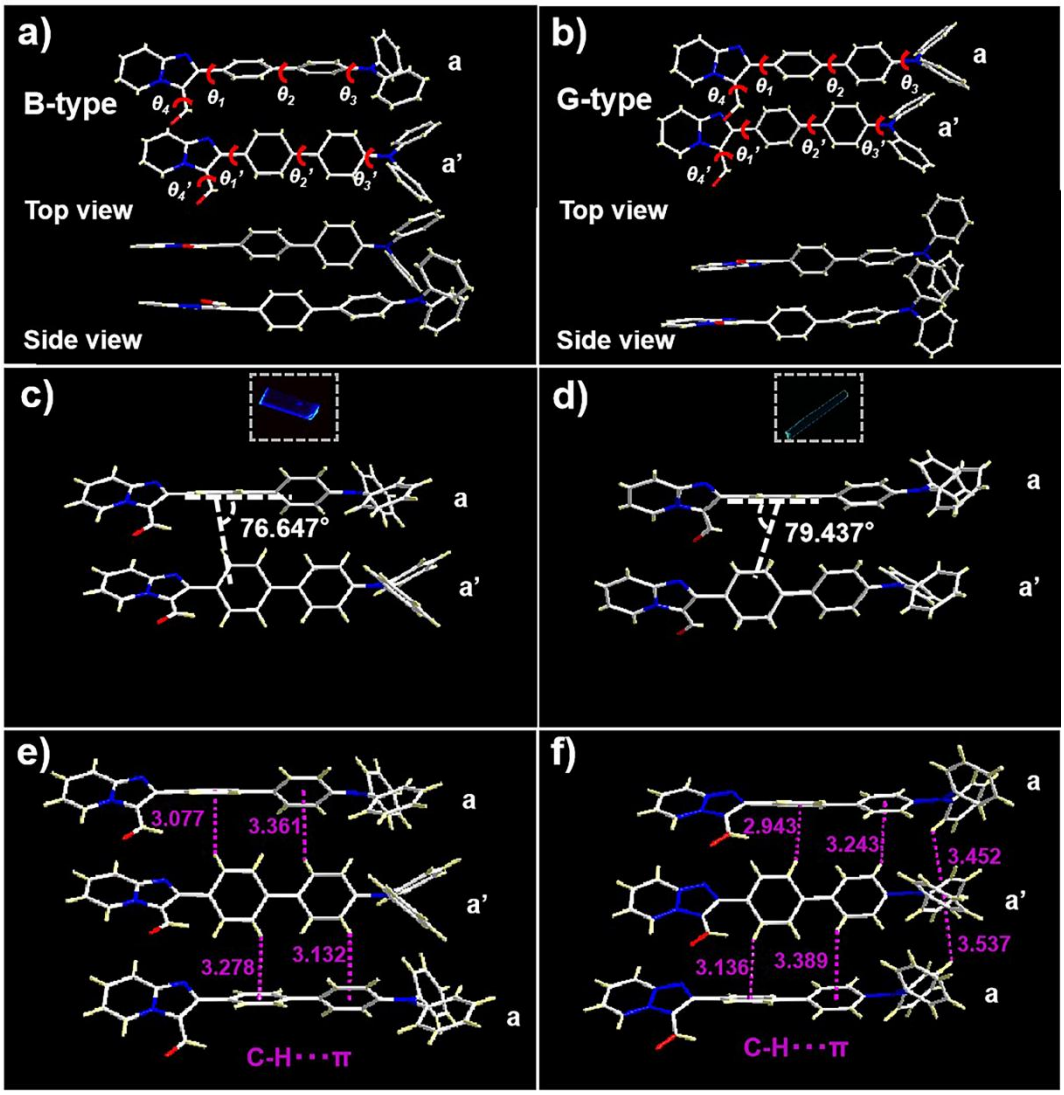

Figure. S25. (a, b) Single crystal packing patterns of B-type, G-type. (c, d) Packing patterns between the upper and lower layers. (e, f) Packing patterns and intermolecular forces of individual three-layer molecules. Unit: Å.

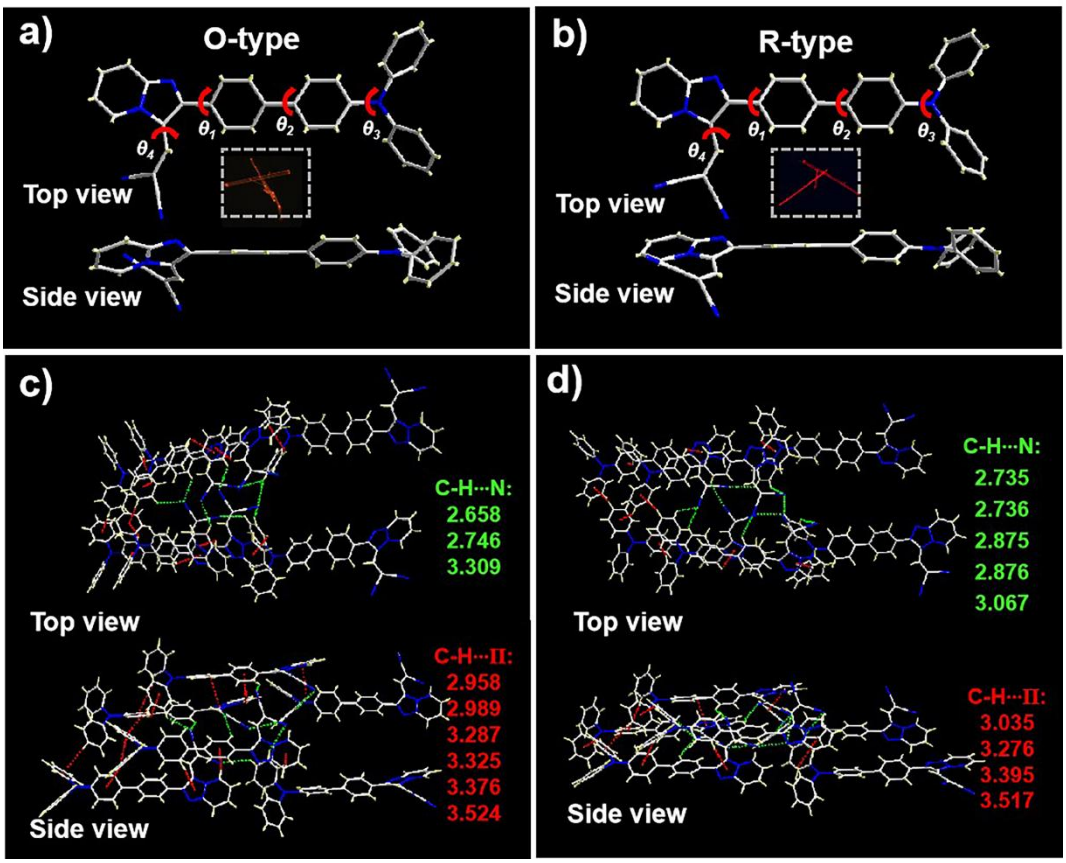

Figure. S26. (a, b) Single crystal packing patterns of O-type, R-type. Intermolecular packing interactions in the crystal of **TPA-IPBCN** (c) O-type and (d) R-type. Unit: Å.

5. Multistimuli-responsive properties

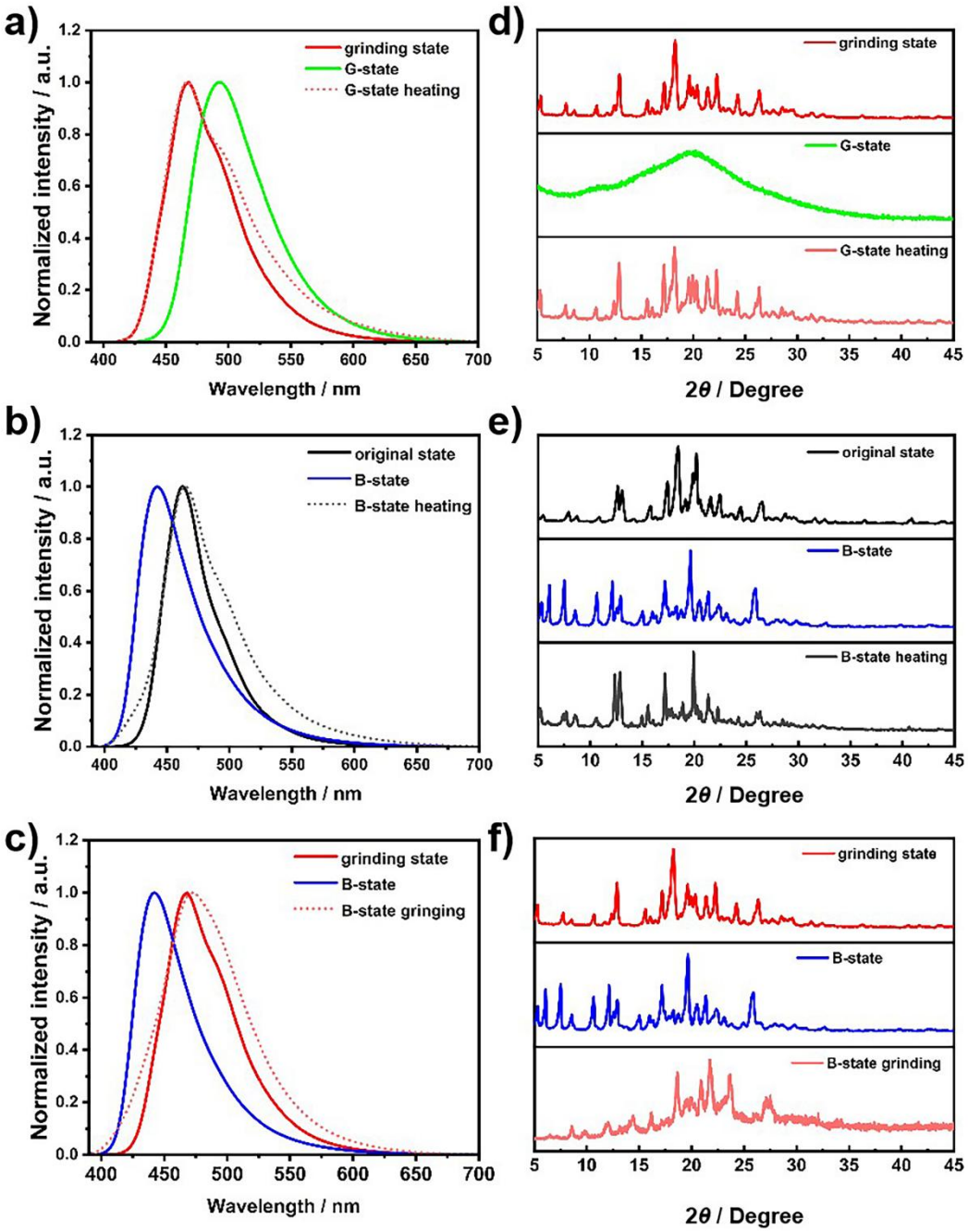

Figure. S27. Normalized emission and PXRD spectra of **TPA-IPBA** transitions in different solid states.

6. Imaging Data

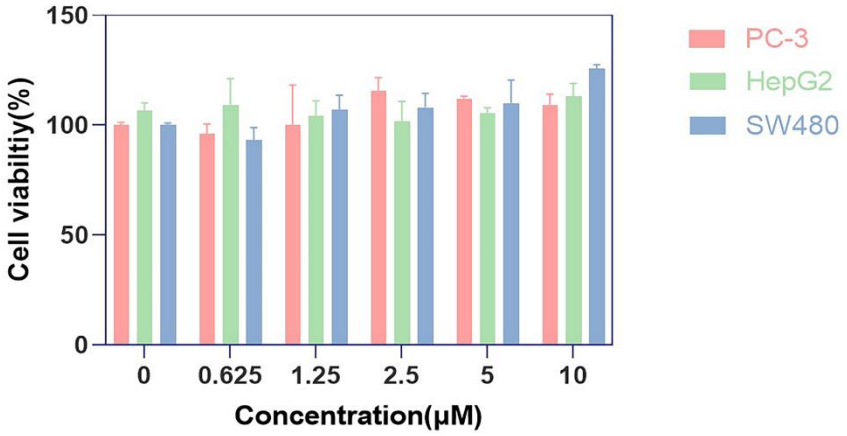

Figure. S28. The cell viability of PC-3, HepG2, and SW480 cells after treatment with probe **TPA-IPBA** after 24 h. The cell viability was obtained via MTT assay.

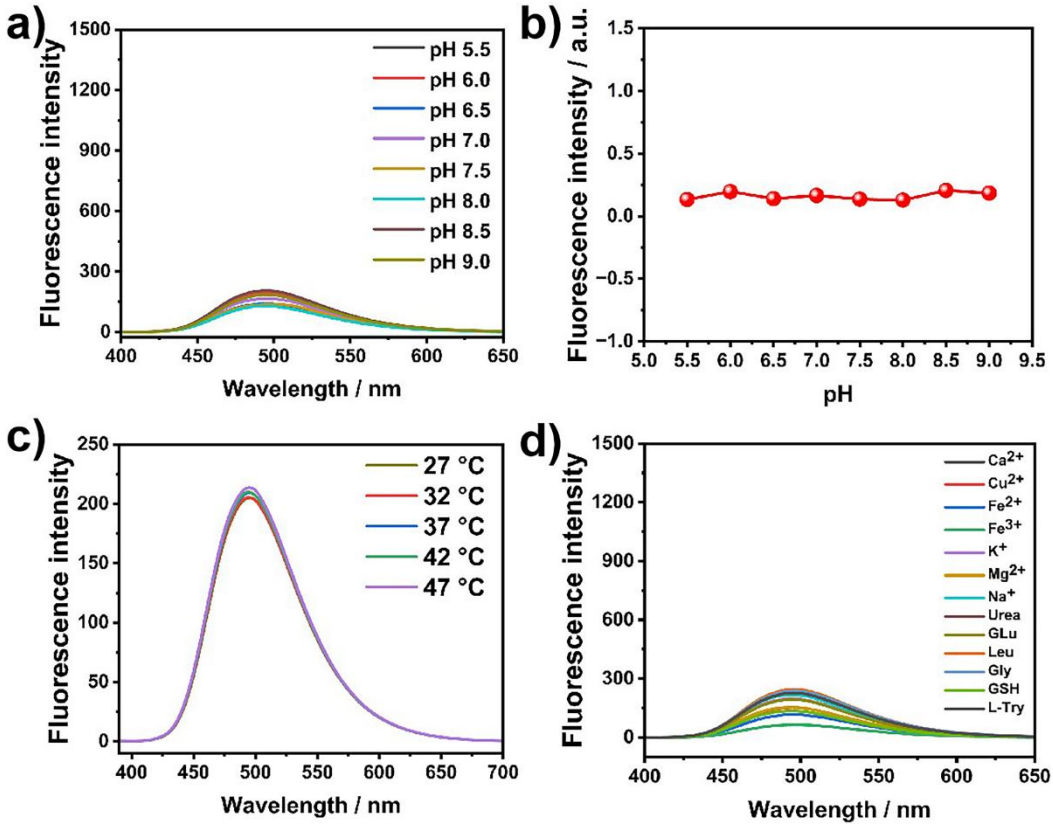

Figure. S29. (a, b) The fluorescence intensity of **TPA-IPBA** (10 μM) in solutions with different pH values. (c) The fluorescence intensity of **TPA-IPBA** (10 μM) in solutions with different temperatures. (d) Fluorescence intensity of **TPA-IPBA** (10 μM) in the presence of Ca^{2+}, Cu^{2+}, Fe^{2+}, Fe^{3+}, K^{+}, Mg^{2+}, Na^{+}, GSH, GLu are 5 mM, Leu, Gly, Urea, L-Try are 1 mM.

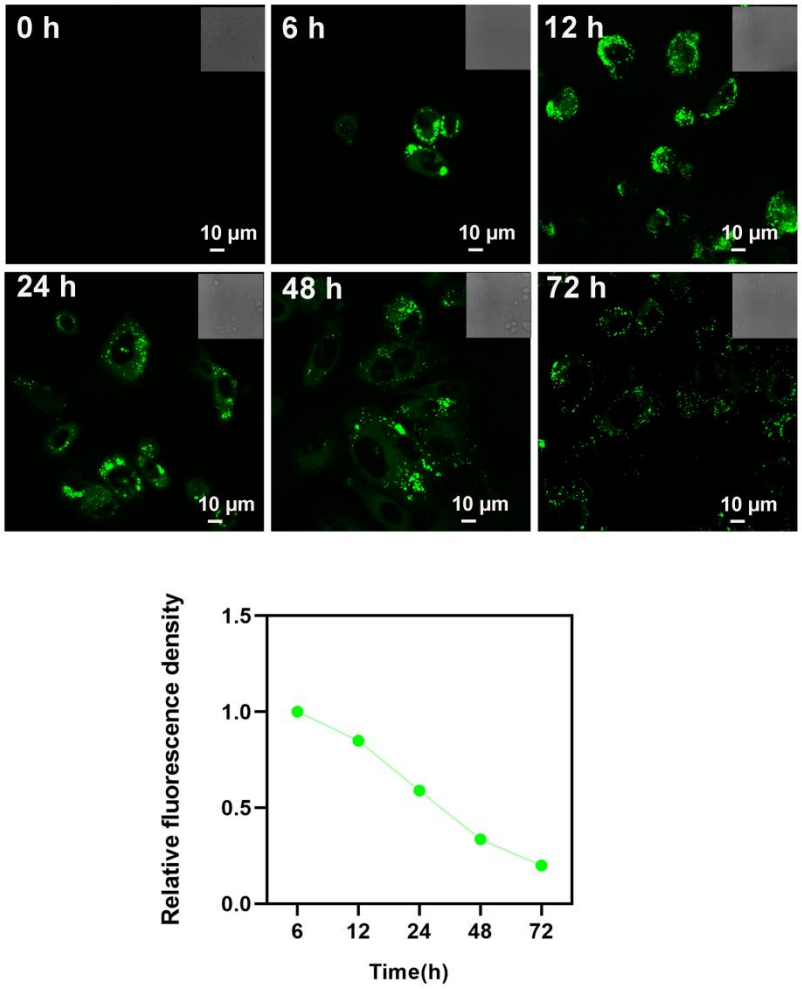

Figure. S30. CLSM imaging after co incubation of **TPA-IPBA** (5 μM) with PC-3 cells for 0 h, 6 h, 12 h, 24 h, 48 h, 72 h, $\lambda_{ex}/\lambda_{em}$ = 405/425-500 nm. Inset: Bright-field images.

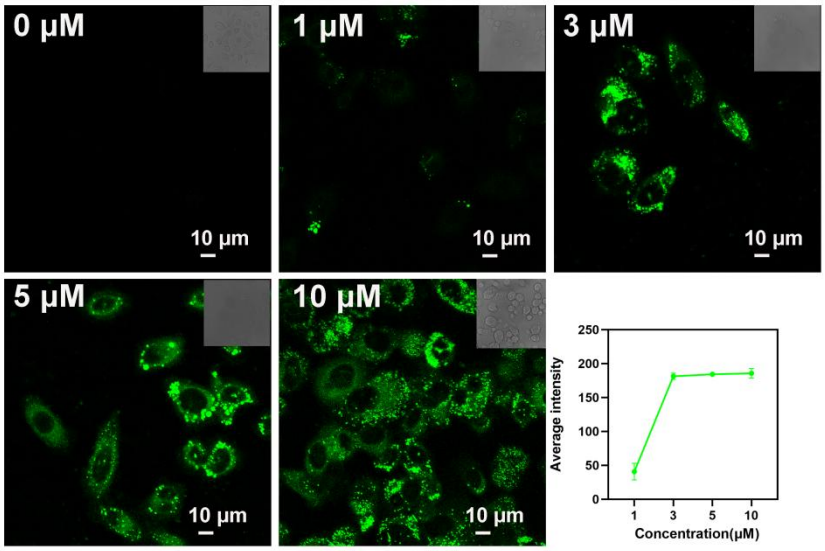

Figure. S31. CLSM imaging after co incubation of **TPA-IPBA** (0 μM, 1 μM, 3 μM, 5 μM, 10 μM)

with PC-3 cells for 30 min, $\lambda_{ex}/\lambda_{em}$ = 405/425-500 nm. Inset: Bright-field images.

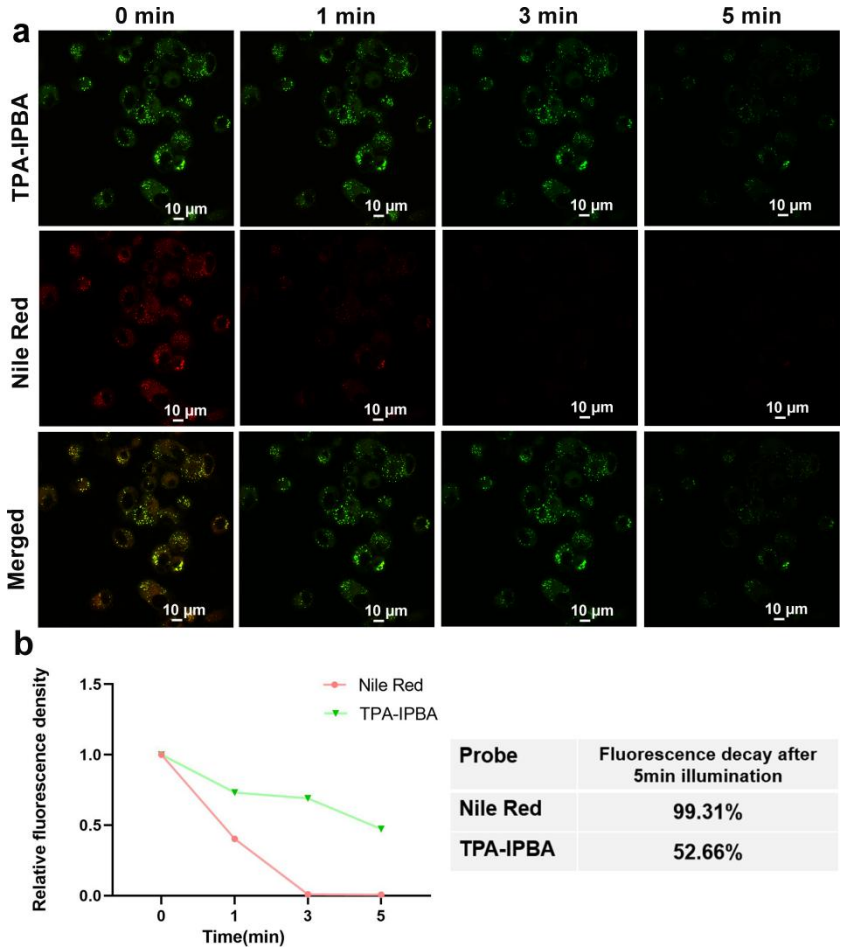

Figure. S32. (a) Images of **TPA-IPBA** (5 μM) and Nile Red (5 μM) at 0, 1, 3, and 5 min in PC-3 cells under continuous laser (405 nm and 488 nm laser) irradiation, Image of **TPA-IPBA** ($\lambda_{ex}/\lambda_{em}$ = 405/425-500 nm), Image of Nile Red ($\lambda_{ex}/\lambda_{em}$ = 488/500-750 nm); (b) Quantification of fluorescence intensity decay for **TPA-IPBA** and Nile Red.

Table S7. Lipid droplets size statistics (μm).

LDs number	1	2	3	4	5	6	7	8	9	10	average
Control	0.67	0.68	0.89	0.7	0.72	0.88	0.68	0.89	0.69	0.97	**0.777**
+Oleic acid	1.75	1.84	2.04	2	1.75	2.09	2.17	2.83	2.34	2.09	**2.09**

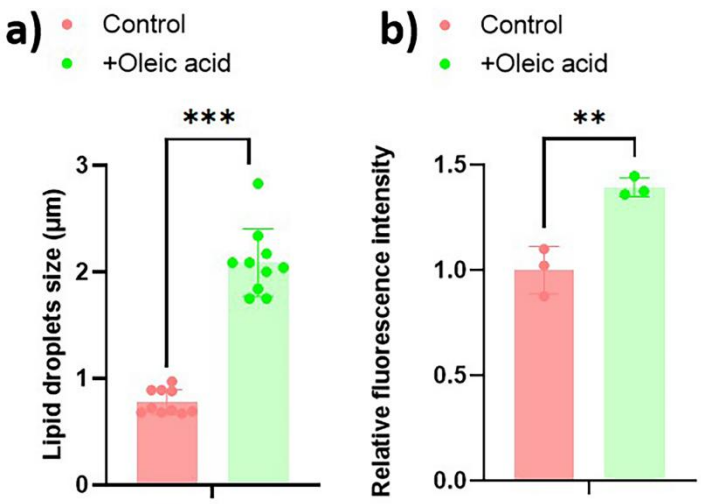

Figure. S33. (a) Lipid droplets size statistics and (b) relative fluorescence intensity.

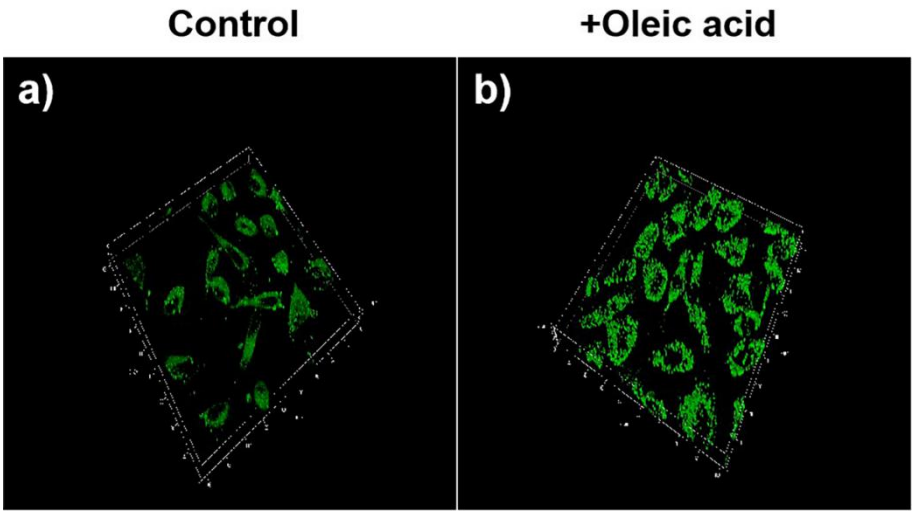

Figure. S34. 3D CLSM imaging of PC-3 cells with **TPA-IPBA** (5 μM). (a) Without oleic acid added. (b) Cells were incubated with oleic acid (500 μM) for 3 h, then incubated with **TPA-IPBA** for 30 min. $\lambda_{ex}/\lambda_{em}$ = 405/425-500 nm.

Table S8. Comparison between **TPA-IPBA** and other similar DSE materials.

Molecular structure	**$\tau^{[a]}$(ns)**	**$\Phi_f{}^{[a]}$[%]**	**$\tau^{[b]}$(ns)**	**$\Phi_f{}^{[b]}$[%]**	**Stimulus-response**
TPA-BT *Dyes Pigm,* **2022**, *198*, 109958.	4.47	58.9	2.8	30.27	Mechanofluorochromism
TPA-BBT *Dyes Pigm,* **2022**, *198*, 109958.	3.28	56.8	2.82	60.92	Mechanofluorochromism

2PB-AC *CCS Chem*, **2023**, *5*, 1686-1696.	2.43	90.2	2.65	92.7	-
2TPACHO *Mol Syst Des Eng*, **2022**, *7*, 963-968.	-	43	2.56	62	Solvatochromism；Mechanofluorochromism
TPA-AN-PhBT *Org Lett*, **2022**, *24*, 8305−8309.	-	1.5	-	26	-
TPA-BT-ANPh *Org Lett*, **2022**, *24*, 8305−8309.	-	93	-	44	-
TPA-QCN *J Phys Chem C*, **2019**, *123*, 24705-24713.	-	34.1	-	19.7	-
4 *Mater Adv*, **2021**, *2*, 996-1005.	-	28	-	12.2	-
5 *Mater Adv*, **2021**, *2*, 996-1005.	-	37	-	11.3	-
6 *Mater Adv*, **2021**, *2*, 996-1005.	-	31	-	15.3	Acidichromism(intensity variation)
NP-TPA *Mater Chem Front*, **2022**, *6*, 155-162.	7.62	58	13.71	51	Solvatochromism
XAO-TPA *JPPA*, **2023**, *443*, 114853.	-	54	-	28.4	Mechanofluorochromism ; Solvatochromism
TPA-IP *Cryst Growth Des*, **2024**, *24*, 3388−3398.	-	7.1	-	1.86	Mechanofluorochromism (intensity variation); Acidichromism

PH-CNTPA *Spectrochim Acta A,* **2024**, *318*, 124474.	-	35	-	34.6	Mechanofluorochromism ; Solvatochromism; Photochromic.
BVDP Chem Commun,2014,50,2569-2571	-	29	-	-	Solvatochromism; Acidichromism; Mechanofluorochromism
DPBT Adv.Funct.Mater.2023,33,2303627.	-	0.21-0.86	-	56.4	Solvatochromism
IP-4TPA Dyes and Pigments 222 (2024) 111882	-	34.01, 40.83, 51.58, 49.87	1.56, 1.19, 1.51, null.	9.96, 23.77, 12.63, null.	Solvatochromism
IP1-5 Dyes and Pigments 224 (2024) 112004	2.984 1.569 2.197 2.562 1.266	42 22 45 10 3	2.196 2.875 2.875 8.925 21.079	6 7 13 27 8	Solvatochromism
TPA-IPBA Our work	2.88	75.91	3.29	38.56	Solvatochromism; Mechanofluorochromism ; Acidichromism; Solid-phase polymorphism